Eur. Phys. J. C (2022) 82:662
https://doi.org/10.1140/epjc/s10052-022-10649-7

THE EUROPEAN PHYSICAL JOURNAL C

Regular Article - Theoretical Physics

Scattering of fermionic isodoublets on the sine-Gordon kink

A. Yu. Loginov[a]

Tomsk State University of Control Systems and Radioelectronics, 634050 Tomsk, Russia

Received: 17 May 2022 / Accepted: 27 July 2022

Abstract The scattering of Dirac fermions on the sine-Gordon kink is studied both analytically and numerically. To achieve invariance with respect to a discrete symmetry, the sine-Gordon model is treated as a nonlinear σ-model with a circular target space that interacts with fermionic isodublets through the Yukawa interaction. It is shown that the diagonal and antidiagonal parts of the fermionic wave function interact independently with the external field of the sine-Gordon kink. The wave functions of the fermionic scattering states are expressed in terms of the Heun functions. General expressions for the transmission and reflection coefficients are derived, and their dependences on the fermion momentum and mass are studied numerically. The existence condition is found for two fermionic zero modes, and their analytical expressions are obtained. It is shown that the zero modes do not lead to fragmentation of the fermionic charge, but can lead to polarization of the fermionic vacuum. The scattering of the diagonal and antidiagonal fermionic states is found to be significantly different; this difference is shown to be due to the different dependences of the energy levels of these bound states on the fermion mass, and is in accordance with Levinson's theorem.

1 Introduction

Many field theory models with spontaneously broken symmetry possess stable localized solutions known as topological solitons [1]. One example of a topological soliton is a kink [2], which is a one-dimensional static solution of a $(1+1)$-dimensional field model. The best known are the kinks of the ϕ^4 [3–5] and the sine-Gordon models [6,7]. The sine-Gordon model has a number of remarkable properties; in particular, it possesses an infinite number of conserved quantities at both the classical and quantum levels. Furthermore, all time-dependent solutions of the sine-Gordon model are known, and can be written down explicitly in closed form. The reason for this is that the sine-Gordon model in $(1+1)$ dimensions is an integrable system. Another special property of the sine-Gordon model is its equivalence to the massive Thirring model, and the quantum soliton of the sine-Gordon model can be identified with the fermion of the massive Thirring model [8].

The sine-Gordon model and its modifications are used in the study of a wide range of phenomena, including QCD [9–11], condensed matter physics [12], and solid state physics in relation to the Josephson junctions and their associated magnetism and topological excitations [13–16]. Models of the sine-Gordon type are also used to describe vortex dynamics in superconducting systems [17] and to investigate the Josephson current in some systems [18].

The interaction between fermions and the background fields of topological solitons leads to a number of interesting physical effects, such as fragmentation of the fermionic number and polarization of the fermionic vacuum [19–22], superconductivity [23], and monopole catalysis of the proton decay [24–27]. In the case of a kink, fragmentation of the fermionic number and polarization of the fermionic vacuum are possible [19]. In addition, the kink's field distorts the energy levels of the fermionic vacuum; bound states can arise and continuum states can change compared to a free fermion. These lead to a change in the zero-point fermion energy, and consequently to the Casimir effect, in the presence of the kink [28].

Various aspects of the interaction of fermions with kinks, kink-antikink configurations, and domain walls were considered in Refs. [29–48]. The main purpose of the present work is to study the scattering and bound states of fermions in the external field of the sine-Gordon kink. A characteristic property of the sine-Gordon model is its invariance with respect to discrete equidistant shifts of a scalar field. The usual Yukawa interaction of a fermion with the scalar field will break this discrete $\mathbb{Z}$-symmetry of the sine-Gordon model, and in order to avoid this, the sine-Gordon model is treated as a nonlinear

[a] e-mail: a.yu.loginov@tusur.ru (corresponding author)

Published online: 02 August 2022

σ-model whose target space is a circle, and the scalar field is treated as an angular variable. Under these conditions, the Yukawa interaction of the σ-model's two-component nonlinear scalar field with a fermionic isodoublet will not break the discrete $\mathbb{Z}$-symmetry.

This paper is structured as follows. In Sect. 2, we describe briefly the Lagrangian, symmetries, field equations, and kink solution of the sine-Gordon model. In Sect. 3, we consider fermion-kink scattering, and derive analytical expressions for the fermionic scattering states and general expressions for the transmission and reflection coefficients. In Sect. 4, we study the fermionic bound states: the general properties of the fermionic bound states are described, and their symmetries under the charge conjugation and parity transformations are established. A condition for the existence of the fermionic zero modes is found, and the properties of these modes are studied. In Sect. 5, we present numerical results relating to the fermion-kink interaction. In the final section, we briefly summarize the results obtained in this work. Appendix A contains some necessary information on the plane-wave states of free fermions, and Appendix B gives an explanation of the dependence of the energy of the fermionic bound state on the fermion mass at a qualitative level.

Throughout the paper, the natural units $c = 1$ and $\hbar = 1$ are used.

2 Lagrangian, symmetries, and field equations of the model

The Lagrangian density of the $(1 + 1)$-dimensional sine-Gordon model has the form

$$\mathcal{L} = \frac{1}{2}\partial_\mu\phi\partial^\mu\phi - m^4\lambda^{-1}\big(1 - \cos\big(m^{-1}\lambda^{1/2}\phi\big)\big), \tag{1}$$

where $\phi(t, x)$ is a real scalar field, m is the mass of the ϕ-meson, and λ is the self-interaction coupling constant of the real scalar field ϕ. The Lagrangian $L = \int \mathcal{L}dx$ possesses symmetries under the two discrete transformations:

$$\bar{\phi}\,(t, x) \to -\bar{\phi}\,(t, x)\,, \tag{2}$$

and

$$\bar{\phi}\,(t, x) \to \bar{\phi}\,(t, x) + 2\pi N,\ \ N \in \mathbb{Z}, \tag{3}$$

where the rescaled scalar field $\bar{\phi} = m^{-1}\lambda^{1/2}\phi$. According to these symmetries, the classical vacua of model (1) are located at the points

$$\bar{\phi}\,(t, x) = 2\pi N,\ \ N \in \mathbb{Z}, \tag{4}$$

which correspond to the zero minima of the potential $U\left(\bar{\phi}\right) = 1 - \cos\left(\bar{\phi}\right)$. It follows from Eqs. (3) and (4) that the field $\bar{\phi} = m^{-1}\lambda^{1/2}\phi$ may be interpreted as an angular variable, defined modulo 2π. We want the Lagrangian to remain invariant under discrete transformations (3) when fermions are included in the sine-Gordon model, and it is obvious that the usual version of the Yukawa interaction $\bar{\psi}\phi\psi$ does not satisfy this requirement.

The interpretation of $\bar{\phi}$ as an angular variable makes it possible to formulate the sine-Gordon model as a nonlinear σ model whose target space is a circle [1]. To do this, we introduce the two-component isovector scalar field

$$\boldsymbol{\phi} = (\phi_1, \phi_2) = \left(m\lambda^{-1/2}\cos\left(\bar{\phi}\right),\ m\lambda^{-1/2}\sin\left(\bar{\phi}\right)\right), \tag{5}$$

which is invariant under discrete transformations (3). We want the interaction between the Dirac fermionic field and isovector scalar field (5) to also be invariant under transformations (3). This is most naturally achieved through the Yukawa interaction $\boldsymbol{\phi}\cdot\bar{\psi}\boldsymbol{\tau}_\perp\psi$, where $\boldsymbol{\tau}_\perp = (\tau_1, \tau_2)$ and $\tau_{1,2}$ are the corresponding Pauli matrices. Indeed, the $SO(2)$ isovector $\bar{\psi}\boldsymbol{\tau}_\perp\psi$ is also invariant under the 2π rotation about the third isotopic axis, as is the $SO(2)$ isovector $\boldsymbol{\phi}$. Moreover, the term $\boldsymbol{\phi}\cdot\bar{\psi}\boldsymbol{\tau}\psi$ is invariant under the full $SU(2)$ isotopic group, and hence the term $\boldsymbol{\phi}\cdot\bar{\psi}\boldsymbol{\tau}_\perp\psi$ is invariant under the $U(1)$ subgroup of the $SU(2)$ isotopic group that corresponds to isotopic rotations about the third axis.

In terms of the isovector field $\boldsymbol{\phi}$, the Lagrangian density of the sine-Gordon model including an isodublet of the Dirac fermions takes the form

$$\begin{aligned}\mathcal{L} = {} & \frac{1}{2}\partial_\mu\boldsymbol{\phi}\cdot\partial^\mu\boldsymbol{\phi} - m^4\lambda^{-1}\big(1 - m^{-1}\lambda^{1/2}\phi_1\big) \\ & + \frac{\nu}{2}\left(\boldsymbol{\phi}\cdot\boldsymbol{\phi} - m^2\lambda^{-1}\right) + i\bar{\psi}\gamma^\mu\partial_\mu\psi - g\boldsymbol{\phi}\cdot\bar{\psi}\boldsymbol{\tau}_\perp\psi,\end{aligned} \tag{6}$$

where the Lagrange multiplier ν is introduced to constrain $\boldsymbol{\phi}$ to lie on the circle $\boldsymbol{\phi}\cdot\boldsymbol{\phi} = m^2\lambda^{-1}$. It is understood that the two types of indices of the Dirac field ψ_{ia} correspond to its spinor-isospinor structure. In $(1+1)$ dimensions, we use the following Dirac matrices:

$$\gamma^0 = \sigma_1,\ \ \gamma^1 = -i\sigma_2,\ \ \gamma_5 = \gamma^0\gamma^1 = \sigma_3, \tag{7}$$

where σ_i are the Pauli matrices. To distinguish the Pauli matrices σ_k acting on the spinor index i of the fermionic field ψ_{ia} from those acting on its isospinor index a, we denote the latter as τ_k.

It is readily seen that the Lagrangian density (6) is invariant under discrete $\mathbb{Z}$-transformations (3). It is also invariant under discrete $\mathbb{Z}_2$-transformation (2) provided that the Dirac fermionic field ψ_{ia} is transformed as $\psi \to \mathbb{I}\otimes\tau_3\psi$. By varying the action $S = \iint \mathcal{L}dxdt$ in the corresponding fields, we

obtain the field equations:

$$\partial_\mu \partial^\mu \boldsymbol{\phi} - m^3 \lambda^{-1/2} \mathbf{n}_1 - \nu \boldsymbol{\phi} + g \bar{\psi} \boldsymbol{\tau}_\perp \psi = 0, \tag{8}$$

and

$$i \gamma^\mu \partial_\mu \psi - g \boldsymbol{\phi} \cdot \boldsymbol{\tau}_\perp \psi = 0, \tag{9}$$

where the Lagrange multiplier

$$\nu = m^{-2} \lambda \left(\boldsymbol{\phi} \cdot \partial_\mu \partial^\mu \boldsymbol{\phi} - m^3 \lambda^{-1/2} \boldsymbol{\phi} \cdot \mathbf{n}_1 + g \boldsymbol{\phi} \cdot \bar{\psi} \boldsymbol{\tau}_\perp \psi \right) \tag{10}$$

and the unit isovector $\mathbf{n}_1 = (1, 0)$.

It is known that that among the numerous soliton solutions, the sine-Gordon model possesses the static kink solution

$$\phi_{\mathrm{k}}(x) = 4 m \lambda^{-1/2} \arctan \left[\exp (mx) \right] \tag{11}$$

or in terms of the isovector field

$$\boldsymbol{\phi}_{\mathrm{k}}(x) = m \lambda^{-1/2} \Big(1 - 2 \mathrm{sech}^2 (mx), \\ -2 \mathrm{sech} (mx) \tanh (mx) \Big). \tag{12}$$

The sine-Gordon kink has mass

$$M_{\mathrm{k}} = 8 m^3 \lambda^{-1}. \tag{13}$$

Note that the mass of the kink is inversely proportional to the self-interaction coupling constant, which is a characteristic property of soliton solutions [49].

We shall now establish the symmetry properties of the Dirac equation (9) under the discrete C, P, and T transformations in the case of external field of kink solution (12). It is easy to see that the kink solution has the symmetry property

$$\phi_{\mathrm{k}i} (x) = (-1)^{i-1} \phi_{\mathrm{k}i} (-x), \tag{14}$$

where $i = 1, 2$ is the component number of the isovector $\boldsymbol{\phi}_{\mathrm{k}}$. Using this symmetry property, it can easily be shown that if $\psi(t, x)$ is a solution of the Dirac equation (9) in the external field of kink (12), then

$$\psi^C (t, x) = \eta_C \gamma_5 \otimes \tau_1 \psi^* (t, x), \tag{15a}$$
$$\psi^P (t, x) = \eta_P \gamma^0 \otimes \tau_1 \psi (t, -x), \tag{15b}$$
$$\psi^T (t, x) = \eta_T \gamma^0 \otimes \tau_1 \psi^* (-t, x), \tag{15c}$$

where η_C, η_P, and η_T are phase multipliers, are also solutions of the Dirac equation in the external field of the kink.

When the fermion backreaction is taken into account, the kink solution (12) becomes perturbed and may depend on time. In this case, Eqs. (15a)–(15c) must be supplemented by appropriate transformations of the scalar field

$$\phi_i^C (t, x) = \phi_i (t, x), \tag{16a}$$
$$\phi_i^P (t, x) = (-1)^{i-1} \phi_i (t, -x), \tag{16b}$$
$$\phi_i^T (t, x) = \phi_i (-t, x). \tag{16c}$$

Taking into account anticommutativity of the fermionic field ψ, it can easily be shown that the action $S = \iint \mathcal{L}(t, x)\, dt dx$ is invariant under the C, P, and T transformations given by Eqs. (15) and (16). It follows that field equations (8) and (9) are also invariant under these transformations, which is easy to check by direct calculation.

The antikink solution is obtained from kink solution (12) through the inversion $x \to -x$. Using the symmetry property (14), it can easily be shown that if $\psi_{\mathrm{k}}(t, x)$ is a solution of the Dirac equation (9) in the external field of kink (12), then

$$\psi_{\mathrm{ak}} (t, x) = \mathbb{I} \otimes \tau_1 \psi_{\mathrm{k}} (t, x) \tag{17}$$

is a solution of the Dirac equation (9) in the external field of the antikink $\boldsymbol{\phi}_{\mathrm{ak}}(x) = \boldsymbol{\phi}_{\mathrm{k}}(-x)$.

As $x \to \pm\infty$, isovector kink field (12) tends to the vacuum value

$$\lim_{x \to \pm\infty} \boldsymbol{\phi}_{\mathrm{k}} (x) = \boldsymbol{\phi}_{\mathrm{vac}} = \left(m \lambda^{-1/2}, 0 \right). \tag{18}$$

It follows that in the distant spatial regions $|x| \gg m^{-1}$, the Dirac equation (9) describes free fermions (antifermions) with mass $M = mg\lambda^{-1/2}$. The properties of the corresponding plane-wave solutions of the Dirac equation and their explicit forms are given in Appendix A.

3 Fermion-kink scattering

We shall consider fermion scattering on the sine-Gordon kink (12) in the external field approximation. In this approximation, the backreaction of a fermion on the field of the kink is neglected, and kink-soliton scattering is described solely by the Dirac equation (9). To neglect the fermion backreaction, the contribution of the fermionic terms in Eqs. (8) and (10) should be much less than that of the corresponding bosonic terms. Using normalization condition (A.4c) to estimate the contribution of the fermionic terms, it can be shown that the condition of their smallness has the form

$$g^2 \ll m^2 \varepsilon L, \tag{19}$$

where ε is the fermion energy and L is the normalized length. In the nonrelativistic case, condition (19) becomes more stringent:

$$g^2 \ll m^2 M L = g m^2 \lambda^{-1/2} m L, \tag{20}$$

where the fermion mass $M = mg\lambda^{-1/2}$.

We see that conditions (19) and (20) can always be fulfilled if the normalized length L is sufficiently large, corresponding to a low linear density of the incident fermions. From the

viewpoint of QFT, however, we are talking about the scattering of a fermion of mass $M = mg\lambda^{-1/2}$ on a sine-Gordon kink of mass $M_{\rm k} = 8m^3\lambda^{-1}$. To neglect the recoil of the kink in fermion scattering, the mass of the kink $M_{\rm k}$ must be much larger than the mass of the fermion M, which leads to the condition

$$\varkappa \equiv gm^{-2}\lambda^{1/2}/8 = (gm^{-1})(\lambda^{1/2}m^{-1})/8 \ll 1. \tag{21}$$

By comparing Eqs. (20) and (21), we see that they are equivalent if the normalization length $L \approx 8m^{-1}$. In turn, it follows from Eq. (11) that the value of $8m^{-1}$ can be interpreted as the spatial size of the kink. Hence, Eqs. (20) and (21) become equivalent when there is on average one fermion in a region whose length is equal to the spatial size of the kink.

The classical solution (12) adequately describes the kink only if it is in the semi-classical regime, which means that the dimensionless combination $\lambda^{-1/2}m^{-1}$ is small. The smallness of $\lambda^{-1/2}m^{-1}$ means that the contribution of quantum bosonic corrections is small, with the result that the leading-order quantum correction $-m/\pi$ to the classical kink mass $M_{\rm k} = 8m^3\lambda^{-1}$ is much less than $M_{\rm k}$ itself. For a correct description of the fermion-kink system by field equations (8) and (9), the smallness of the other dimensionless combination gm^{-1} is also necessary, since this means the smallness of quantum fermionic corrections. Thus, for a correct description of the fermion-kink system by Eqs. (8) and (9), it is necessary to satisfy the weak coupling conditions

$$\lambda^{1/2}m^{-1} \ll 1 \quad \text{and} \quad gm^{-1} \ll 1. \tag{22}$$

We see that the fulfillment of the weak coupling conditions results in the fulfillment of condition (21), which means the applicability of the external field approximation.

Substituting the ansatz $\psi_{ia}(t,x) = \exp(-i\varepsilon t)\,\psi_{ia}(x)$ and background kink field (12) into the Dirac equation (9), we obtain the two independent systems of differential equations:

$$\begin{pmatrix}\psi_{11}'\\ \psi_{22}'\end{pmatrix} = \begin{pmatrix} i\varepsilon & -iMF(x)\\ iMF^*(x) & -i\varepsilon\end{pmatrix}\begin{pmatrix}\psi_{11}\\ \psi_{22}\end{pmatrix} \tag{23}$$

and

$$\begin{pmatrix}\psi_{12}'\\ \psi_{21}'\end{pmatrix} = \begin{pmatrix} i\varepsilon & -iMF^*(x)\\ iMF(x) & -i\varepsilon\end{pmatrix}\begin{pmatrix}\psi_{12}\\ \psi_{21}\end{pmatrix}, \tag{24}$$

where the unitary function

$$\begin{aligned} F(x) &= \left(\frac{e^{mx}+i}{e^{mx}-i}\right)^2 \\ &= 1 - 2\,\mathrm{sech}^2(mx) + 2i\,\mathrm{sech}(mx)\tanh(mx). \end{aligned} \tag{25}$$

The Dirac equation (9) can be split into the two independent subsystems (23) and (24) since the Dirac Hamiltonian

$$H_D = \alpha\otimes\mathbb{I}\,(-i\partial_x) + g\beta\otimes\boldsymbol{\phi}_{\rm k}\cdot\boldsymbol{\tau}_\perp \tag{26}$$

commutes with the spin-isospin operator $T_3 = \gamma_5\otimes\tau_3$:

$$[H_D, T_3] = 0. \tag{27}$$

Here, Eq. (23) contains only the diagonal elements of the matrix ψ_{ia}, whereas Eq. (24) contains only the antidiagonal ones. Let us denote the diagonal and antidiagonal parts of the matrix ψ_{ia} as $\psi_{\rm d}$ and $\psi_{\rm a}$, respectively:

$$\psi_{\rm d} = \begin{pmatrix}\psi_{11} & 0\\ 0 & \psi_{22}\end{pmatrix}, \quad \psi_{\rm a} = \begin{pmatrix}0 & \psi_{12}\\ \psi_{21} & 0\end{pmatrix}. \tag{28}$$

It can then be easily shown that $\psi_{\rm d}$ and $\psi_{\rm a}$ are the eigenmatrices of the operator T_3:

$$T_3\psi_{\rm d} = \psi_{\rm d}, \quad T_3\psi_{\rm a} = -\psi_{\rm a}. \tag{29}$$

It follows from Eqs. (27) and (29) that $\psi_{\rm d}$ and $\psi_{\rm a}$ are independent from each other, and this is reflected in Eqs. (23) and (24).

It can be shown that system (23) is equivalent to the second-order differential equation

$$\begin{aligned} &\psi_{11}''(x) + 2im\,\mathrm{sech}(mx)\psi_{11}'(x) \\ &\quad + \left(k^2 + 2\varepsilon m\,\mathrm{sech}(mx)\right)\psi_{11}(x) = 0 \end{aligned} \tag{30}$$

together with the relation

$$\psi_{22}(x) = M^{-1}F^*(x)\left(\varepsilon\psi_{11}(x) + i\psi_{11}'(x)\right), \tag{31}$$

where $k^2 = \varepsilon^2 - M^2$. Specifically, any solution to system (23) satisfies Eqs. (30) and (31). Conversely, the function $\psi_{11}(x)$ that satisfies Eq. (30) together with the function $\psi_{22}(x)$ obtained from Eq. (31) form a solution to system (23). Indeed, in the latter case, the derivative ψ_{22}' satisfies the relation

$$\psi_{22}'(x) = M^{-1}F^*(x)\left(\varepsilon\psi_{11}'(x) - ik^2\psi_{11}(x)\right), \tag{32}$$

where we use Eq. (30) to eliminate ψ_{11}''. It is easy to see that by substituting Eqs. (31) and (32) into system (23), the latter is identically satisfied. Similarly, system (24) is equivalent to the second-order differential equation

$$\begin{aligned} &\psi_{12}''(x) - 2im\,\mathrm{sech}(mx)\psi_{12}'(x) \\ &\quad + \left(k^2 - 2\varepsilon m\,\mathrm{sech}(mx)\right)\psi_{12}(x) = 0 \end{aligned} \tag{33}$$

together with the relation

$$\psi_{21}(x) = M^{-1}F(x)\left(\varepsilon\psi_{12}(x) + i\psi_{12}'(x)\right). \tag{34}$$

By applying a change of variable $\xi = \tanh(mx)$, the second-order differential equations (30) and (33) are reduced to the forms

$$\psi_{11}''(\xi) - \frac{2\left(\xi - i\sqrt{1-\xi^2}\right)}{1-\xi^2}\psi_{11}'(\xi) + \frac{\left(k^2 + 2\varepsilon m\sqrt{1-\xi^2}\right)}{m^2\left(1-\xi^2\right)^2}\psi_{11}(\xi) = 0 \tag{35}$$

and

$$\psi_{12}''(\xi) - \frac{2\left(\xi + i\sqrt{1-\xi^2}\right)}{1-\xi^2}\psi_{12}'(\xi) + \frac{\left(k^2 - 2\varepsilon m\sqrt{1-\xi^2}\right)}{m^2\left(1-\xi^2\right)^2}\psi_{12}(\xi) = 0. \tag{36}$$

The solutions to differential Eqs. (35) and (36) can be expressed in terms of the local Heun functions [50,51]. Let the fermionic wave fall on the kink from the left. Then, as $x \to +\infty$, the solutions to Eqs. (35) and (36) must approximate the transmitted plane wave, which is $\propto \exp(ikx)$. In terms of the initial variable x, the corresponding solutions to Eqs. (35) and (36) are

$$\psi_{11}(x) = e^{ikx} Hl\left[\frac{1}{2}, -i\frac{2(\varepsilon - k)}{m}; -1, 0, 1 - i\frac{2k}{m}, 1 + i\frac{2k}{m}; \frac{1}{1 + ie^{mx}}\right] \tag{37}$$

and

$$\psi_{12} = e^{-\frac{\pi}{2}\frac{k}{m}}\left[e^{-i\frac{\pi}{4}} + e^{i\frac{\pi}{4}}e^{-mx}\right]^{2i\frac{k}{m}} e^{ikx} \times Hl\left[\frac{1}{2}, -2\frac{k^2}{m^2} - i\frac{2\varepsilon - k}{m}; -1 - i\frac{2k}{m}, -i\frac{2k}{m}, 1 - i\frac{2k}{m}, 1 - i\frac{2k}{m}; \frac{1}{1 - ie^{mx}}\right], \tag{38}$$

where we use the notation $Hl(a, q; \alpha, \beta, \gamma, \delta; z)$ for the six-parameter local Heun function [50,51].

The local Heun function $Hl(a, q; \alpha, \beta, \gamma, \delta; z)$ represents the solution to the second-order differential Heun's equation [50,51]. Heun's equation possesses four regular singular points located at $z = 0$, $z = 1$, $z = a$, and $z = \infty$. In Eqs. (37) and (38), the arguments of the local Heun functions tend to zero (one of the regular singular points) as $x \to +\infty$. The local Heun function $Hl(a, q; \alpha, \beta, \gamma, \delta; z)$ is analytic, and is equal to one at the regular singular point $z = 0$, where it can be expanded in a Taylor series. In the complex z-plane, the radius of convergence of this series is equal to the smallest of $|a|$ and one. It follows from Eqs. (37) and (38) that in our case, it is equal to $1/2$.

Despite the finite radius of convergence of the series, the local Heun function $Hl(1/2, q; \alpha, \beta, \gamma, \delta; z)$ can be analytically continued to the whole complex plane with the cut $[1/2, \infty)$. It will be defined at all finite points of the complex plane except for the regular singular points $z = 1/2$ and $z = 1$. At the same time, in Eqs. (37) and (38), the arguments of the local Heun functions tend to one as $x \to -\infty$, and hence local solutions (37) and (38) cannot be used as $x \to -\infty$.

It is known [50,51], however, that Heun's equation has another local solution such that the local Heun functions entering it will be analytic in the neighborhood of the singular point $z = 1$. The same is also true for the solutions to Eqs. (35) and (36). Specifically, it can be shown that the solutions ψ_{11} and ψ_{12} can be represented in the alternative forms

$$\psi_{11}(x) = c_1 e^{ikx} Hl\left[\frac{1}{2}, i\frac{2(\varepsilon - k)}{m}; -1, 0, 1 + i\frac{2k}{m}, 1 - i\frac{2k}{m}; \frac{1}{1 - ie^{-mx}}\right] + c_2 e^{-ikx}\left(-i + e^{mx}\right)^{2i\frac{k}{m}} \times Hl\left[\frac{1}{2}, -2\frac{k^2}{m^2} + i\frac{2\varepsilon + k}{m}; -1 - i\frac{2k}{m}, -i\frac{2k}{m}, 1 - i\frac{2k}{m}, 1 - i\frac{2k}{m}; \frac{1}{1 - ie^{-mx}}\right] \tag{39}$$

and

$$\psi_{12} = d_1 e^{-\pi\frac{k}{m}} e^{ikx}\left(i + e^{mx}\right)^{-2i\frac{k}{m}} \times Hl\left[\frac{1}{2}, -2\frac{k^2}{m^2} + i\frac{2\varepsilon - k}{m}; -1 + i\frac{2k}{m}, i\frac{2k}{m}, 1 + i\frac{2k}{m}, 1 + i\frac{2k}{m}; \frac{1}{1 + ie^{-mx}}\right] + d_2 e^{-\pi\frac{k}{m}} e^{-ikx} \times Hl\left[\frac{1}{2}, i\frac{2(k + \varepsilon)}{m}; -1, 0, 1 - i\frac{2k}{m}, 1 + i\frac{2k}{m}; \frac{1}{1 + ie^{-mx}}\right], \tag{40}$$

where c_1, c_2, d_1, and d_2 are constant coefficients. Now the arguments of the local Heun functions tend to zero as $x \to -\infty$, meaning that the local Heun functions remain analytic in this limit. Forms (37) and (39) of the solution ψ_{11} have overlapping domains of analyticity in the variable x. The same is also true for forms (38) and (40) of the solution ψ_{12}. It follows that by equating the alternative expressions for $\psi_{11}(x)$ and its derivative $d\psi_{11}(x)/dx$, we can find the coefficients c_1 and c_2 in Eq. (39), and in Eq. (40), the coefficients d_1 and d_2 can be found in a similar way. The x-coordinate of the matching point does not matter, and can lie in the interval $(-\infty, \infty)$. For reasons of symmetry, we choose the coordinate of the matching point as $x = 0$. In

this case, the coefficients c_1 and c_2 can be written as ratios of bilinear combinations:

$$c_1 = \left\{-m\left[\chi'_{\rm tr}\left(s^*\right)\chi_{\rm rf}\left(s\right)+\chi_{\rm tr}\left(s^*\right)\chi'_{\rm rf}\left(s\right)\right] +4sk\chi_{\rm tr}\left(s^*\right)\chi_{\rm rf}\left(s\right)\right\}V\left(s\right)^{-1}, \tag{41}$$

$$c_2 = 2^{-i\frac{k}{m}}e^{-\frac{\pi}{2}\frac{k}{m}}m\left[\chi'_{\rm tr}\left(s^*\right)\chi_{\rm in}\left(s\right) +\chi_{\rm tr}\left(s^*\right)\chi'_{\rm in}\left(s\right)\right]V\left(s\right)^{-1} \tag{42}$$

where the functions

$$\chi_{\rm in}\left(z\right) = Hl\left[\frac{1}{2},i\frac{2\left(\varepsilon-k\right)}{m};-1,0, 1+i\frac{2k}{m},1-i\frac{2k}{m};z\right], \tag{43}$$

$$\chi_{\rm rf}\left(z\right) = Hl\left[\frac{1}{2},-2\frac{k^2}{m^2}+i\frac{2\varepsilon+k}{m};-1-i\frac{2k}{m}, -i\frac{2k}{m},1-i\frac{2k}{m},1-i\frac{2k}{m};z\right], \tag{44}$$

$$\chi_{\rm tr}\left(z\right) = Hl\left[\frac{1}{2},-i\frac{2\left(\varepsilon-k\right)}{m};-1,0, 1-i\frac{2k}{m},1+i\frac{2k}{m};z\right], \tag{45}$$

the bilinear combination

$$V\left(s\right) = 4sk\chi_{\rm rf}\left(s\right)\chi_{\rm in}\left(s\right)+mW\left(s\right), \tag{46}$$

the Wronskian

$$W\left(s\right) = \left[\chi_{\rm rf}\left(z\right)\chi'_{\rm in}\left(z\right)-\chi'_{\rm rf}\left(z\right)\chi_{\rm in}\left(z\right)\right]_{z=s}, \tag{47}$$

and the argument $s=\left(1+i\right)/2$. Similarly, the coefficients d_1 and d_2 are

$$d_1 = -2^{2i\frac{k}{m}}\left\{-m\left[\eta'_{\rm tr}\left(s\right)\eta_{\rm rf}\left(s^*\right)+\eta_{\rm tr}\left(s\right)\eta'_{\rm rf}\left(s^*\right)\right] +4sk\eta_{\rm tr}\left(s\right)\eta_{\rm rf}\left(s^*\right)\right\}U\left(s^*\right)^{-1}, \tag{48}$$

$$d_2 = 2^{i\frac{k}{m}}e^{\frac{\pi}{2}\frac{k}{m}}\left\{-m\left[\eta'_{\rm tr}\left(s\right)\eta_{\rm in}\left(s^*\right)+\eta_{\rm tr}\left(s\right)\eta'_{\rm in}\left(s^*\right)\right] +4k\eta_{\rm tr}\left(s\right)\eta_{\rm in}\left(s^*\right)\right\}U\left(s^*\right)^{-1}, \tag{49}$$

where the functions

$$\eta_{\rm in}\left(z\right) = Hl\left[\frac{1}{2},-2\frac{k^2}{m^2}+i\frac{2\varepsilon-k}{m};-1+i\frac{2k}{m}, i\frac{2k}{m},1+i\frac{2k}{m},1+i\frac{2k}{m};z\right], \tag{50}$$

$$\eta_{\rm rf}\left(z\right) = Hl\left[\frac{1}{2},i\frac{2\left(k+\varepsilon\right)}{m};-1,0, 1-i\frac{2k}{m},1+i\frac{2k}{m};z\right], \tag{51}$$

$$\eta_{\rm tr}\left(z\right) = Hl\left[\frac{1}{2},-2\frac{k^2}{m^2}-i\frac{2\varepsilon-k}{m};-1-i\frac{2k}{m}, -i\frac{2k}{m},1-i\frac{2k}{m},1-i\frac{2k}{m};z\right], \tag{52}$$

the bilinear combination

$$U\left(s^*\right) = 4s^*k\eta_{\rm rf}\left(s^*\right)\eta_{\rm in}\left(s^*\right)-mW\left(s^*\right), \tag{53}$$

the Wronskian

$$W\left(s^*\right) = \left[\eta_{\rm rf}\left(z\right)\eta'_{\rm in}\left(z\right)-\eta'_{\rm rf}\left(z\right)\eta_{\rm in}\left(z\right)\right]_{z=s^*}, \tag{54}$$

and the argument $s^*=\left(1-i\right)/2$. In Eqs. (41)–(54), the subscripts "in", "rf", and "tr" refer to the incident, transmitted, and reflected fermionic wave, respectively.

The coefficients c_1 and c_2 (d_1 and d_2) contain all the information about the scattering of the diagonal (antidiagonal) component $\psi_{\rm d}$ ($\psi_{\rm a}$) of the fermionic wave on the sine-Gordon kink. It follows from Eqs. (37) and (39) that the asymptotics of scattering for the ψ_{11} component can be schematically represented as

$$c_1e^{ikx}\rightarrow e^{ikx}+c_2e^{\pi\frac{k}{m}}e^{-ikx}, \tag{55}$$

which corresponds to the splitting of the incident wave into the transmitted and reflected waves. Next, using Eq. (31) for the ψ_{22} component and the expression $j^\mu=\bar{\psi}\gamma^\mu\otimes\mathbb{I}\psi=\left(\psi^*\psi,\psi^*\sigma_3\otimes\mathbb{I}\psi\right)$ for the fermionic current, we obtain expressions for the incident, transmitted, and reflected currents of the diagonal component $\psi_{\rm d}$:

$$j_{\rm in} = c_1c_1^*\left(1-M^{-2}\left(\varepsilon-k\right)^2\right), \tag{56}$$

$$j_{\rm rf} = c_2c_2^*e^{2\pi\frac{k}{m}}\left(1-M^{-2}\left(\varepsilon+k\right)^2\right), \tag{57}$$

$$j_{\rm tr} = 1-M^{-2}\left(\varepsilon-k\right)^2. \tag{58}$$

Using Eqs. (56)–(58), we obtain expressions for the transmission and reflection coefficients:

$$T = \frac{j_{\rm tr}}{j_{\rm in}} = \left|c_1\right|^{-2}, \tag{59}$$

$$R = \frac{\left|j_{\rm rf}\right|}{j_{\rm in}} = \frac{\left|c_2\right|^2}{\left|c_1\right|^2}e^{2\pi\frac{k}{m}}\left(1+2M^{-2}k\left(\varepsilon+k\right)\right), \tag{60}$$

which correspond to the scattering of the diagonal component $\psi_{\rm d}$ on the sine-Gordon kink. In the process of scattering, the transmitted diagonal fermionic wave acquires a phase shift $\delta_{\rm d}$ with respect to the incident diagonal fermionic wave. Eq. (55) tells us that this phase shift

$$\delta_{\rm d}(k) = -\arg[c_1(k)]. \tag{61}$$

In a similar way to Eq. (55), the scattering of the ψ_{12} component can be schematically written as

$$d_1e^{ikx}\rightarrow e^{ikx}+d_2e^{-\pi\frac{k}{m}}e^{-ikx}. \tag{62}$$

In the same way as above, we can sequentially obtain expressions for the fermionic currents:

$$j_{\rm in} = d_1 d_1^* \left(1 - M^{-2}\,(\varepsilon - k)^2\right), \tag{63}$$

$$j_{\rm rf} = d_2 d_2^* e^{-2\pi \frac{k}{m}} \left(1 - M^{-2}\,(\varepsilon + k)^2\right), \tag{64}$$

$$j_{\rm tr} = 1 - M^{-2}\,(\varepsilon - k)^2\,, \tag{65}$$

and the corresponding transmission and reflection coefficients:

$$T = \frac{j_{\rm tr}}{j_{\rm in}} = |d_1|^{-2}\,, \tag{66}$$

$$R = \frac{|j_{\rm rf}|}{j_{\rm in}} = \frac{|d_2|^2}{|d_1|^2} e^{-2\pi \frac{k}{m}} \left(1 + 2M^{-2} k\,(\varepsilon + k)\right). \tag{67}$$

Equations (63)–(67) correspond to the scattering of the antidiagonal component $\psi_{\rm a}$ on the sine-Gordon kink. From Eq. (62), it follows that when the antidiagonal component $\psi_{\rm a}$ is scattered, the phase shift

$$\delta_{\rm a}(k) = -\arg[d_1(k)]. \tag{68}$$

Let us now define the mean value of the isospin x-projection I_1 for a plane-wave fermionic state as

$$\langle I_1 \rangle = \frac{1}{2} \frac{\psi^* \mathbb{I} \otimes \tau_1 \psi}{\psi^* \mathbb{I} \otimes \mathbb{I} \psi}. \tag{69}$$

It follows from Eq. (69) that the mean value $\langle I_1 \rangle$ of the isospin x-projection lies in the interval $[-1/2, 1/2]$, and is relativistically invariant, as it should be. It can easily be shown that the mean value $\langle I_1 \rangle$ vanishes identically for the both the diagonal and antidiagonal fermionic states:

$$\langle I_1 \rangle_{\rm d,\,in} = \langle I_1 \rangle_{\rm d,\,rf} = \langle I_1 \rangle_{\rm d,\,tr} = 0, \tag{70}$$

$$\langle I_1 \rangle_{\rm a,\,in} = \langle I_1 \rangle_{\rm a,\,rf} = \langle I_1 \rangle_{\rm a,\,tr} = 0. \tag{71}$$

However, for a linear combination $\alpha \psi_{\rm d} + \beta \psi_{\rm a}$, the mean value $\langle I_1 \rangle$ is different from zero. In particular, it can be shown that

$$\langle I_1 \rangle_{\rm in} = \frac{{\rm Re}\left[\alpha^* \beta\right]}{|\alpha|^2 + |\beta|^2}, \tag{72}$$

$$\langle I_1 \rangle_{\rm tr} = \frac{{\rm Re}\left[\alpha^* \beta c_1 d_1^*\right]}{|\alpha d_1|^2 + |\beta c_1|^2}, \tag{73}$$

$$\langle I_1 \rangle_{\rm rf} = \frac{{\rm Re}\left[\alpha^* \beta c_1 c_2^* d_1^* d_2\right]}{e^{-2\pi \frac{k}{m}} |\alpha c_2 d_1|^2 + e^{2\pi \frac{k}{m}} |\beta c_1 d_2|^2} \tag{74}$$

for the incident, reflected, and transmitted waves of the scattering state $\alpha \psi_{\rm d} + \beta \psi_{\rm a}$, respectively.

4 Fermionic bound states

Let us investigate the presence of fermionic bound states in the external field of the sine-Gordon kink. It is obvious that the energy ε of a fermionic bound state must be less than the fermion mass M. In this case, the parameter $k^2 = \varepsilon^2 - M^2$ becomes negative: $k^2 \equiv -\kappa^2 < 0$. It then follows from Eqs. (30), (31), (33), and (34) that the components of the wave function of a fermionic bound state are $\propto \exp(-\kappa\,|x|)$ as $|x| \to \infty$. Next, it is easily shown that under charge conjugation (15a), the diagonal fermionic wave function becomes an antidiagonal one, and vice versa. Since the charge conjugation reverses the sign of the energy of the fermionic state, the bound states of the Dirac Hamiltonian (26) can be split into pairs, each consisting of diagonal and antidiagonal bound states with opposite energies and connected to each other by charge conjugation (15a).

Further, it can be shown that the Dirac Hamiltonian (26), parity operator (15b), and operator T_3 (27) commute with each other. It follows that the parity transformation leaves the type (diagonal or antidiagonal) of a fermionic state unchanged. At the same time, it is known that one-dimensional bound states are nondegenerate [52]. By combining these facts, we can conclude that diagonal and antidiagonal bound states should possess certain parities.

We first consider a diagonal fermionic bound state $\psi_{\rm d}$. In Eq. (37), the argument of the local Heun function tends to zero as $x \to \infty$, and hence the local Heun function tends to unity. It follows that under the replacement $k \to i\kappa$, the transmitted fermionic wave will have the correct bound state asymptotics $\propto \exp(-\kappa x)$ as $x \to \infty$. Under the replacement $k \to i\kappa$ in Eq. (39), the reflected wave also will have the correct asymptotics $\propto \exp(\kappa x)$ as $x \to -\infty$; however, in Eq. (39), the incident wave will then be $\propto \exp(-\kappa x)$ and will increase indefinitely as $x \to -\infty$. To eliminate the incorrect asymptotic behavior of the incident fermionic wave in Eq. (39), the coefficient $c_1(\varepsilon, k)$ must vanish at $\varepsilon = \varepsilon_n, k = i\kappa_n = i\left(M^2 - \varepsilon_n^2\right)^{1/2}$, where ε_n is the energy of a diagonal bound state. Note that the coefficient $c_1(\varepsilon, k)$ is explicitly determined by Eq. (41) and Eqs. (43)–(47). Thus, the energy levels ε_n of the diagonal fermionic bound states are determined by the solutions of the transcendental equation

$$c_1\left(\varepsilon, i\left(M^2 - \varepsilon^2\right)^{1/2}\right) = 0. \tag{75}$$

Similarly, we can conclude that the energy levels of the antidiagonal fermionic bound states are determined by the transcendental equation

$$d_1\left(\varepsilon, i\left(M^2 - \varepsilon^2\right)^{1/2}\right) = 0, \tag{76}$$

where the coefficient $d_1(\varepsilon, k)$ is explicitly determined by Eq. (48) and Eqs. (50)–(54). Due to the symmetry of the Dirac equation under charge conjugation (15a), the energy levels of the diagonal (antidiagonal) antifermionic bound

states are opposite in sign to those of the antidiagonal (diagonal) fermionic bound states.

As in the case of fermion scattering, the wave functions of the bound states described above are the result of matching two local analytic solutions of Eq. (30) (or Eq. (33)) at some intermediate point. At the same time, there are bound states whose wave functions are analytic in the entire complex plane, excluding the point at infinity. To demonstrate this, we consider Eq. (37). As mentioned above, after the replacement $k \to i\kappa$, Eq. (37) will show the correct asymptotic behavior $\propto \exp(-\kappa x)$ as $x \to \infty$. However, the factor $\exp(-\kappa x)$ increases indefinitely as $x \to -\infty$, whereas at large negative x, the correct asymptotics of the bound state should be $\propto \exp(\kappa x)$. Hence, to compensate for the unlimited growth of the factor $\exp(-\kappa x)$ and to obtain the correct (i.e., $\propto \exp(\kappa x)$) asymptotic behavior of the bound state, the local Heun function in Eq. (37) must tend to zero as $\exp(2\kappa x)$, as $x \to -\infty$. The argument of the local Heun function entering Eq. (37) tends to unity as $x \to -\infty$. It follows that the local Heun function should be analytic in the vicinity of unity.

Recall that Heun's equation has four regular singular points at $z = 0$, $z = a$, $z = 1$, and $z = \infty$. The local Heun function $Hl(a, q; \alpha, \beta, \gamma, \delta; z)$ is analytic in the vicinity of the regular singular point $z = 0$, but in the general case, it is not defined in the vicinity of the regular singular points $z = a$ and $z = 1$. However, if a local Heun function is analytic in the vicinity of $z = 0$ and $z = 1$, it must also be analytic in the vicinity of $z = a = 1/2$, since the regular singular point $z = a = 1/2$ lies between the other two regular singular points $z = 0$ and $z = 1$. The situation in which the local Heun function $Hl(a, q; \alpha, \beta, \gamma, \delta; z)$ is analytic in a domain containing the three adjacent singularities $z = 0$, $z = a$, and $z = 1$ is rather specific. In this case, $Hl(a, q; \alpha, \beta, \gamma, \delta; z)$ is also a solution around the fourth singularity $z = \infty$ and is reduced to the Heun polynomial [50,51]. A necessary condition for this is $\alpha = -n$, where n is a positive integer. Note that the local Heun functions in Eq. (37) have the parameter $\alpha = -1$.

When $\alpha = -n$, where n is a positive integer, the $(n+1)$-th coefficient in the series expansion of the local Heun function $Hl(a, q; \alpha, \beta, \gamma, \delta; z)$ is a polynomial in q of order $n+1$. If q is a root of that polynomial, then the $(n+1)$-th coefficient vanishes and with it all the following ones, so the series is truncated and the local Heun function becomes the Heun polynomial. In our case, the series expansion of the local Heun function in Eq. (37) has the form

$$Hl\left[\frac{1}{2}, -\frac{2(\kappa + i\varepsilon)}{m}; -1, 0, 1 + \frac{2\kappa}{m}, 1 - \frac{2\kappa}{m}; z\right] = 1 - \frac{4i(\varepsilon - i\kappa)}{m + 2\kappa} z - \frac{4\varepsilon(\varepsilon - i\kappa)}{(m + \kappa)(m + 2\kappa)} z^2 + O\left(z^3\right), \tag{77}$$

where the parameter $\kappa = \left(M^2 - \varepsilon^2\right)^{1/2}$. We see that in Eq. (77), the coefficient of z^2 vanishes iff the energy $\varepsilon = 0$. In this case, the local Heun function (77) is reduced to the first-order Heun polynomial

$$Hp_{1,1}[1/2, -2M/m; -1, 0, 1 + 2M/m, 1 - 2M/m; z] = 1 - 4M(m + 2M)^{-1} z. \tag{78}$$

The Heun polynomial vanishes at the regular singular point $z = 1$ iff the following condition holds

$$m = 2M, \tag{79}$$

which is equivalent to the condition

$$g\lambda^{-1/2} = 1/2. \tag{80}$$

We conclude that in the external field of the sine-Gordon kink, the diagonal bound state with zero energy (diagonal zero mode) exists iff condition (79) holds. Similarly, it can be shown that this is also true for the antidiagonal zero mode. In this case, the analytic wave function arises from the reflected wave in Eq. (40), and the local Heun function entering the reflected wave also has the parameter $\alpha = -1$.

Let us denote the diagonal and antidiagonal zero modes as ψ_{0d} and ψ_{0a}, respectively. These zero modes can then be written in the form

$$\psi_{0d} = \sqrt{\frac{2}{\pi i}} M^{1/2} \begin{pmatrix} -\dfrac{e^{Mx}}{1 + ie^{2Mx}} & 0 \\ 0 & \dfrac{e^{Mx}}{i + e^{2Mx}} \end{pmatrix}, \tag{81}$$

$$\psi_{0a} = \sqrt{\frac{2}{\pi i}} M^{1/2} \begin{pmatrix} 0 & \dfrac{e^{Mx}}{i + e^{2Mx}} \\ \dfrac{e^{Mx}}{1 + ie^{2Mx}} & 0 \end{pmatrix}. \tag{82}$$

The zero modes (81) and (82) are normalized to unity and become $\propto \exp(-M|x|)$ as $|x| \to \infty$.

We now investigate the properties of the zero modes (81) and (82) under the charge conjugation (15a) and parity transformation (15b). Choosing the phase factors η_C and η_P to be equal to 1 and -1, respectively, we find that

$$\psi_{0d}^C(t, x) = \psi_{0a}(t, x), \tag{83}$$

$$\psi_{0a}^C(t, x) = \psi_{0d}(t, x), \tag{84}$$

$$\psi_{0d}^P(t, x) = \psi_{0d}(t, x), \tag{85}$$

$$\psi_{0a}^P(t, x) = -\psi_{0a}(t, x). \tag{86}$$

We see that the diagonal and antidiagonal zero modes turn into each other under the C-conjugation. We also see that these zero modes are the eigenstates of the parity operator P, and that their eigenvalues (i.e., parities) are opposite. Later, from our numerical results, we shall see that the antidiagonal

and diagonal zero modes should be regarded as fermionic and antifermionic, respectively.

Using the zero modes $\psi_{0\mathrm{d}}$ and $\psi_{0\mathrm{a}}$, we can form even and odd linear combinations:

$$\psi_{0\mathrm{e}} = 2^{-1/2}\left(\psi_{0\mathrm{d}} + \psi_{0\mathrm{a}}\right), \tag{87}$$

$$\psi_{0\mathrm{o}} = i2^{-1/2}\left(\psi_{0\mathrm{d}} - \psi_{0\mathrm{a}}\right), \tag{88}$$

which are the eigenstates of the C-conjugation operator

$$\psi_{0\mathrm{e}}^{C}(t,x) = \psi_{0\mathrm{e}}(t,x), \tag{89}$$

$$\psi_{0\mathrm{o}}^{C}(t,x) = \psi_{0\mathrm{o}}(t,x). \tag{90}$$

At the same time, the zero modes $\psi_{0\mathrm{e}}$ and $\psi_{0\mathrm{o}}$ turn into each other up to a phase factor under the parity transformation

$$\psi_{0\mathrm{e}}^{P}(t,x) = -i\psi_{0\mathrm{o}}(t,x), \tag{91}$$

$$\psi_{0\mathrm{o}}^{P}(t,x) = i\psi_{0\mathrm{e}}(t,x). \tag{92}$$

Note also that the mean value of the isospin x-projection vanishes for all types of zero modes:

$$\langle I_1\rangle_{\psi_{0\mathrm{d}}} = \langle I_1\rangle_{\psi_{0\mathrm{a}}} = \langle I_1\rangle_{\psi_{0\mathrm{e}}} = \langle I_1\rangle_{\psi_{0\mathrm{o}}} = 0. \tag{93}$$

Equations (89) and (90) tell us that $\psi_{0\mathrm{e}}$ and $\psi_{0\mathrm{o}}$ are the Majorana spinors. Using Eqs. (81), (82), (87), and (88), it can be shown that $\psi_{0\mathrm{e}}$ and $\psi_{0\mathrm{o}}$ satisfy the relation

$$\bar{\psi}_{0\mathrm{e}}\boldsymbol{\tau}_{\perp}\psi_{0\mathrm{e}} = \bar{\psi}_{0\mathrm{o}}\boldsymbol{\tau}_{\perp}\psi_{0\mathrm{o}} = 0. \tag{94}$$

It then follows from Eqs. (8) and (10) that the Majorana fermions corresponding to $\psi_{0\mathrm{e}}$ and $\psi_{0\mathrm{o}}$ have no effect on the field of the kink, meaning that the external field approximation becomes exact in this case.

Note that all results related to the fermionic zero modes were obtained in the external field approximation without taking into account the fermion backreaction on the kink. In addition, quantum corrections were also not taken into account, since the fermion-kink system is described by classical field Eqs. (8) and (9). Therefore, the results obtained are applicable only if weak coupling condition (22) holds and, consequently, condition (21) also holds. Accounting for bosonic (fermionic) quantum corrections will lead to the appearance of a correction term on the order of λm^{-2} (g^2m^{-2}) in the r.h.s. of Eq. (80). Taking the fermion backreaction into account for zero modes (81) and (82) will result in a correction term on the order of $\varkappa = 2^{-3}gm^{-2}\lambda^{1/2}$ in the r.h.s. of Eq. (80). In contrast, Majorana zero modes (87) and (88) have no backreaction on the kink, and therefore the corresponding correction term will be absent in this case. However, in any case, the results obtained become inapplicable in the strong coupling regime, in which $\lambda m^{-2} \gtrsim 1$ and/or $g^2m^{-2} \gtrsim 1$. The reason is that in this case, the corrections to the r.h.s. of Eq. (80) will be of the same order as the main term $1/2$, which makes Eq. (80) inapplicable.

Equations (61) and (68) determine the phase shifts in the scattering of the diagonal and antidiagonal fermionic component, respectively. These phase shifts depend on the magnitude of the fermion's momentum. The difference in the phase shifts $\Delta_{\mathrm{d,a}} = \delta_{\mathrm{d,a}}(0) - \delta_{\mathrm{d,a}}(\infty)$ plays an important role in the theory of scattering [52–54]; in particular, Levinson's theorem [55] establishes a relation between this difference and the number of bound states for a given scattering channel. For a one-dimensional case, Levinson's theorem has the form [56]:

$$\Delta = \pi\left(n_b - 1/2\right), \tag{95}$$

where Δ and n_b are the difference in the phase shifts and the number of bound states in a given scattering channel, respectively. In our case, Levinson's theorem is written as

$$\Delta_{\mathrm{d,a}} = \pi\left(n_{\mathrm{d,a}} - 1/2\right), \tag{96}$$

where n_{d} (n_{a}) is the number of diagonal (antidiagonal) fermionic bound states.

Another well-known field theory kink solution is the kink of the ϕ^4 model [3–5]. Unlike the sine-Gordon kink, the ϕ^4 kink has a single Majorana zero mode that exists for all values of the Yukawa coupling constant. The presence of this zero mode leads to fragmentation of the fermionic charge and polarization of the fermionic vacuum [19]. We now consider the effect of the presence of two zero modes (81) and (82) in the field of the sine-Gordon kink. Recall that these zero modes exist iff condition (79) holds. First, we note that one can take either $\psi_{0\mathrm{a}}$ and $\psi_{0\mathrm{d}}$ or $\psi_{0\mathrm{e}}$ and $\psi_{0\mathrm{o}}$ as the states of zero energy. In the first case, the second quantized fermionic field is written as

$$\Psi(t,x) = b_0\psi_{0\mathrm{a}}(x) + d_0^{\dagger}\psi_{0\mathrm{d}}(x) + \sum_{r\geqslant 1}\left(b_r e^{-i\varepsilon_r t}\psi_{r\mathrm{d}}(x) + d_r^{\dagger}e^{i\varepsilon_r t}\psi_{r\mathrm{a}}(x)\right), \tag{97}$$

where it is understood that the fermion-kink system is placed in an one-dimensional box of large but finite length, so that all fermionic energy levels are discrete. In Eq. (97), the role of the diagonal and antidiagonal zero modes is reversed compared to the corresponding nonzero modes. Our numerical results will show that all nonzero diagonal (antidiagonal) modes are fermionic (antifermionic) and that the situation is reversed for zero modes. The annihilation and creation operators satisfy the anticommutation relations

$$\left\{b_r, b_{r'}^{\dagger}\right\} = \left\{d_r, d_{r'}^{\dagger}\right\} = \delta_{rr'}, \tag{98}$$

where $r, r' = 0, 1, 2, \ldots$. The other anticommutators involving the annihilation and creation operators vanish.

Next, to calculate the operator of the fermionic charge, we use the normally ordered fermionic current

$$j^{\mu} = 2^{-1}\left[\Psi^{\dagger}, \gamma^{0}\gamma^{\mu}\Psi\right]. \tag{99}$$

The corresponding expression for the fermionic charge operator is

$$\begin{aligned} Q &= 2^{-1}\int\left(\Psi^{\dagger}\Psi - \Psi\Psi^{\dagger}\right)dx \\ &= b_0^{\dagger}b_0 - d_0^{\dagger}d_0 + \sum_{r\geqslant 1}\left(b_r^{\dagger}b_r - d_r^{\dagger}d_r\right). \end{aligned} \tag{100}$$

It follows from Eq. (100) that the contributions of the zero modes $\psi_{0\mathrm{a}}$ and $\psi_{0\mathrm{d}}$ to the fermionic charge are completely analogous to those of the nonzero modes. Let us denote the state vectors in the subspace of zero modes by $|n_{\mathrm{a}}, n_{\mathrm{d}}\rangle_{(1)}$, where $n_{\mathrm{a\,(d)}} = 0, 1$ is the occupation number of the antidiagonal (diagonal) zero mode. It then follows from Eqs. (98) and (100) that

$$Q\,|0,0\rangle_{(1)} = 0, \tag{101a}$$
$$Q\,|1,0\rangle_{(1)} = |1,0\rangle_{(1)}\,, \tag{101b}$$
$$Q\,|0,1\rangle_{(1)} = -\,|0,1\rangle_{(1)}\,, \tag{101c}$$
$$Q\,|1,1\rangle_{(1)} = 0. \tag{101d}$$

We see that in the case of the zero modes $\psi_{0\mathrm{a}}$ and $\psi_{0\,\mathrm{d}}$, there is no fermionic charge fragmentation, since all eigenvalues of Q are integers. Furthermore, Eq. (101a) tells us that the sine-Gordon kink does not polarize the fermionic vacuum $|0,0\rangle_{(1)}$ because its fermionic charge vanishes.

Next, we consider the case where zero energy fermions are in the Majorana states $\psi_{0\mathrm{e}}$ and $\psi_{0\mathrm{o}}$. The second quantized fermionic field is then written as

$$\begin{aligned} \Psi(t,x) &= \alpha\psi_{0\mathrm{e}}(x) + \beta\psi_{0\mathrm{o}}(x) \\ &\quad + \sum_{r\geqslant 1}\left(b_r e^{-i\varepsilon_r t}\psi_{r\mathrm{d}}(x) + d_r^{\dagger}e^{i\varepsilon_r t}\psi_{r\mathrm{a}}(x)\right), \end{aligned} \tag{102}$$

where the annihilation operators

$$\alpha = 2^{-1/2}\left(b_0 + d_0^{\dagger}\right), \tag{103a}$$
$$\beta = i2^{-1/2}\left(b_0 - d_0^{\dagger}\right) \tag{103b}$$

satisfy the anticommutation relations

$$\left\{\alpha, \alpha^{\dagger}\right\} = \left\{\beta, \beta^{\dagger}\right\} = 1. \tag{104}$$

Note that Eq. (102) contains only the annihilation operators of the zero modes $\psi_{0\mathrm{e}}$ and $\psi_{0\mathrm{o}}$, and the creation operators of the corresponding zero antimodes are absent. This is because the wave functions of the Majorana zero modes $\psi_{0\mathrm{e}}$ and $\psi_{0\mathrm{o}}$ are invariant under the charge conjugation, and hence the corresponding zero modes and antimodes are the same.

In terms of α and β, the fermionic charge Q has the form

$$Q = \alpha^{\dagger}\alpha + \beta^{\dagger}\beta - 1 + \sum_{r\geqslant 1}\left(b_r^{\dagger}b_r - d_r^{\dagger}d_r\right). \tag{105}$$

We denote the state vectors in the subspace of the Majorana zero modes $\psi_{0\mathrm{e}}$ and $\psi_{0\mathrm{o}}$ by $|n_{\mathrm{e}}, n_{\mathrm{o}}\rangle_{(2)}$. The state vectors $|n_{\mathrm{e}}, n_{\mathrm{o}}\rangle_{(2)}$ are linear combinations of the state vectors $|n_{\mathrm{a}}, n_{\mathrm{d}}\rangle_{(1)}$:

$$|0,0\rangle_{(2)} = |0,1\rangle_{(1)}\,, \tag{106a}$$
$$|1,0\rangle_{(2)} = 2^{-1/2}\left(|0,0\rangle_{(1)} + |1,1\rangle_{(1)}\right), \tag{106b}$$
$$|0,1\rangle_{(2)} = 2^{-1/2}\left(|0,0\rangle_{(1)} - |1,1\rangle_{(1)}\right), \tag{106c}$$
$$|1,1\rangle_{(2)} = |1,0\rangle_{(1)}\,. \tag{106d}$$

From Eqs. (104) and (105), we obtain the relations:

$$Q\,|0,0\rangle_{(2)} = -\,|0,0\rangle_{(2)}\,, \tag{107a}$$
$$Q\,|1,0\rangle_{(2)} = 0, \tag{107b}$$
$$Q\,|0,1\rangle_{(2)} = 0, \tag{107c}$$
$$Q\,|1,1\rangle_{(2)} = |1,1\rangle_{(2)}\,. \tag{107d}$$

We see that as in the previous case, there is no fermionic charge fragmentation. At the same time, it follows from Eq. (107a) that the fermionic charge of the vacuum state is equal to minus one, and hence the sine-Gordon kink polarizes the fermionic vacuum $|0,0\rangle_{(2)}$.

5 Numerical results

It follows from Eqs. (23) and (24) that the Dirac equations for the diagonal and antidiagonal components of the fermionic wave function contain the meson mass m and fermion mass $M = mg\lambda^{-1/2}$ as parameters. Passing to the dimensionless variable $\tilde{x} = mx$, it is easy to show that the solutions to the Dirac equation depend only on the dimensionless variables $\tilde{x} = mx$, $\tilde{M} = M/m$, $\tilde{\varepsilon} = \varepsilon/m$, and $\tilde{k} = k/m$, in accordance with Eqs. (37) – (40). Hence, the meson mass m can be taken equal to unity in numerical calculations, while the calculated values can be presented as functions of the dimensionless fermion momentum $\tilde{k} = k/m$ or mass $\tilde{M} = M/m$. In terms of these dimensionless variables, condition (21) ensuring the applicability of the external field approximation takes the form

$$\tilde{g} \ll 8\tilde{\lambda}^{-1/2}, \tag{108}$$

where $\tilde{g} = g/m$ and $\tilde{\lambda} = \lambda/m^2$. From Eq. (108), it follows that the dimensionless fermion mass $\tilde{M} = \tilde{g}\tilde{\lambda}^{-1/2}$ must be much less than the value of $8\tilde{\lambda}^{-1} = 8\times 10^2$, since we used $\tilde{\lambda} = 10^{-2}$ in the numerical calculations.

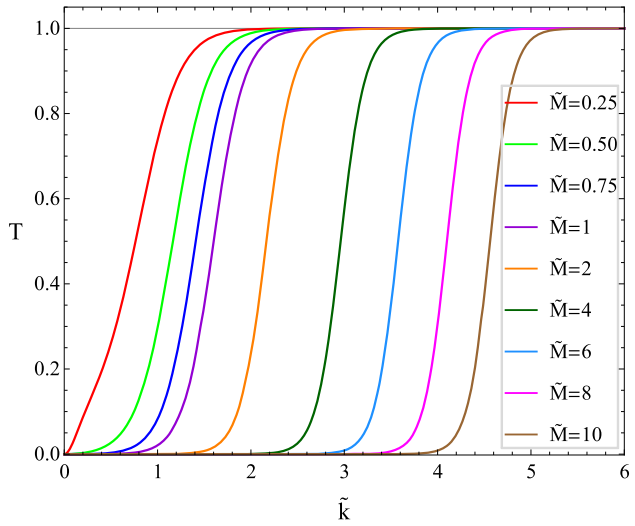

Fig. 1 Dependences of the transmission coefficient T for the antidiagonal component of the fermionic wave function on the fermion momentum $\tilde{k}$ for different values of the fermion mass $\tilde{M}$

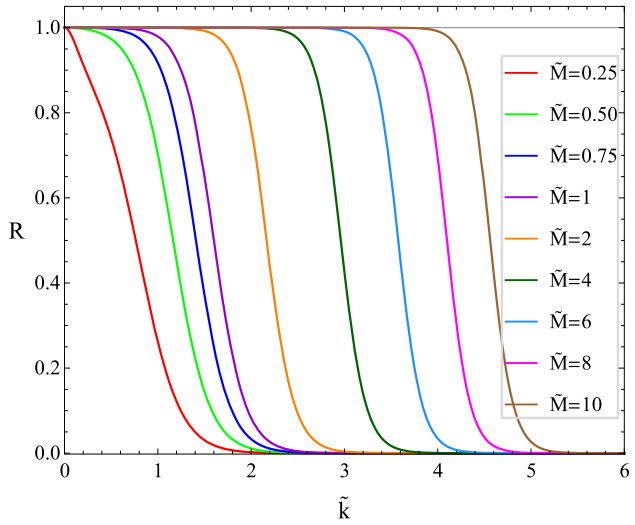

Fig. 2 Dependences of the reflection coefficient R for the antidiagonal component of the fermionic wave function on the fermion momentum $\tilde{k}$ for different values of the fermion mass $\tilde{M}$

Figure 1 presents the dependences of the transition coefficient T for the antidiagonal component of the fermionic wave function on the dimensionless fermion momentum $\tilde{k}$. These dependences were obtained using the analytical expressions in Sect. 3, and are shown for different values of the dimensionless fermion mass $\tilde{M}$. We see that the curves $T(\tilde{k})$ have a characteristic tanh-like shape. As the fermion mass $\tilde{M}$ increases, the curves monotonically shift to the region of larger fermion momenta. Figure 2 shows the curves $R(\tilde{k})$ that correspond to the curves $T(\tilde{k})$ in Fig. 1. It was found that for the same values of $\tilde{M}$, the curves $T(\tilde{k})$ and $R(\tilde{k})$

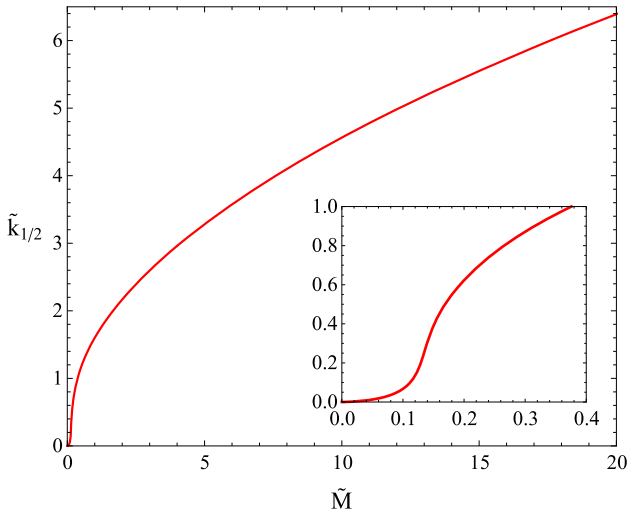

Fig. 3 Dependence of the parameter $\tilde{k}_{1/2}$ on the fermion mass $\tilde{M}$ for the antidiagonal case

satisfy the unitarity condition

$$T(\tilde{k}) + R(\tilde{k}) = 1. \tag{109}$$

Let us define the fermion momentim $\tilde{k}_{1/2}$ by means of the relation $T(\tilde{k}_{1/2}) = R(\tilde{k}_{1/2}) = 1/2$. For a given value of $\tilde{M}$, the value of $\tilde{k}_{1/2}$ determines the position of the midpoints of the curves $T(\tilde{k})$ and $R(\tilde{k})$ in Figs. 1 and 2, respectively. Hence, a fermion with momentum $\tilde{k}_{1/2}$ passes through the kink barrier with probability $1/2$. Figure 3 presents the dependence $\tilde{k}_{1/2}(\tilde{M})$ corresponding to the curves shown in Figs. 1 and 2. It was found numerically that $\tilde{k}_{1/2} \approx 4.2\tilde{M}^2$ for $\tilde{M} \lesssim 0.1$, and $\tilde{k}_{1/2} \approx 1.43\tilde{M}^{1/2}$ for $\tilde{M} \gtrsim 1$. Hence, the fermion velocity $v_{1/2} \approx \tilde{k}_{1/2}/\tilde{M} < 0.1$ if $\tilde{M} < 0.024$. We see that in the antidiagonal case, the fermions that pass through the kink barrier with probability $1/2$ are nonrelativistic when the fermion mass $\tilde{M}$ is small. The fermions also become nonrelativistic for large fermion masses $\tilde{M} > 205$, as in this case, the fermion velocity $v_{1/2} \approx 1.43\tilde{M}^{-1/2} < 0.1$. In the intermediate mass region, the fermions are moderately relativistic.

Next, we turn to the diagonal component of the fermionic wave function. In Figs. 4 and 5 we can see the curves $T(\tilde{k})$ and $R(\tilde{k})$, respectively. These curves carry information about the interaction of the diagonal fermionic component with the sine-Gordon kink. As in the previous case, the curves in Figs. 4 and 5 which correspond to the same $\tilde{M}$ satisfy unitarity condition (109). However, except for this aspect, the behavior of the curves in Figs. 4 and 5 differs substantially from those in Figs. 1 and 2, respectively. In the antidiagonal case (Figs. 1 and 2), the curves $T(\tilde{k})$ and $R(\tilde{k})$ monotonically shift to larger fermion momenta with an increase in the fermion mass $\tilde{M}$. In contrast, in the diagonal case (Figs. 4 and 5), the shift of

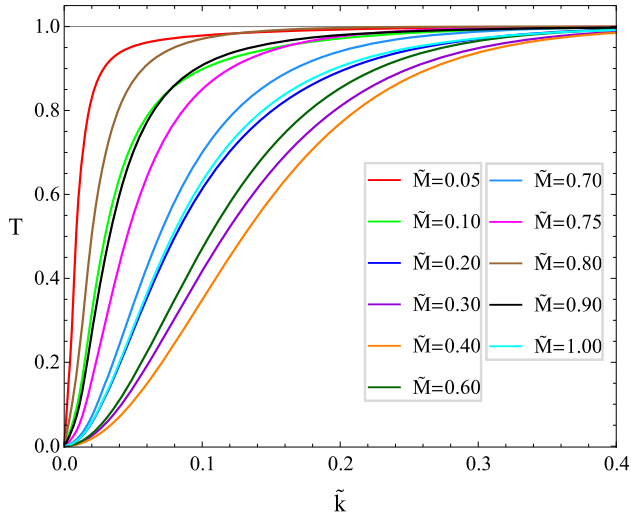

Fig. 4 Dependences of the transmission coefficient T for the diagonal component of the fermionic wave function on the fermion momentum $\tilde{k}$ for different values of the fermion mass $\tilde{M}$

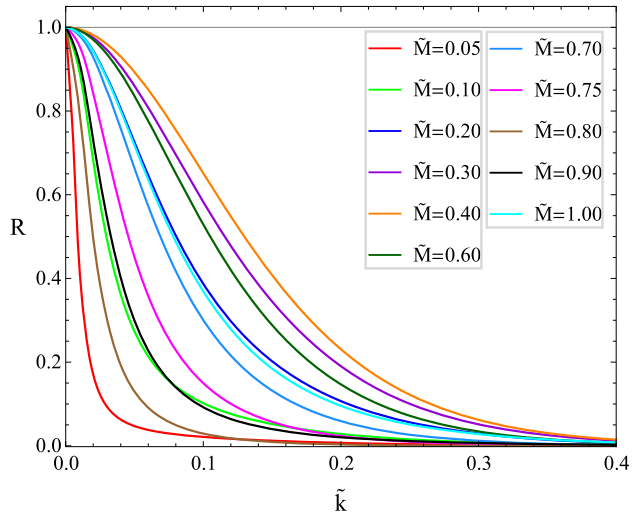

Fig. 5 Dependences of the reflection coefficient R for the diagonal component of the fermionic wave function on the fermion momentum $\tilde{k}$ for different values of the fermion mass $\tilde{M}$

the curves $T(\tilde{k})$ and $R(\tilde{k})$ has an oscillatory character as $\tilde{M}$ increases.

Figure 6 shows the dependence $\tilde{k}_{1/2}(\tilde{M})$ corresponding to the curves in Figs. 4 and 5. We see that the dependences $\tilde{k}_{1/2}(\tilde{M})$ are completely different in the antidiagonal and diagonal cases. The curve $\tilde{k}_{1/2}(\tilde{M})$ monotonically increases in the antidiagonal case in Fig. 3, whereas it has an oscillatory character in the diagonal case in Fig. 6. The amplitude of the oscillations is approximately 0.14, and the oscillation period increases with the fermion mass $\tilde{M}$. In particular, it was found that for $n \gtrsim 3$, the position $\tilde{M}_n$ of the n-th minimum of the curve $\tilde{k}_{1/2}(\tilde{M})$ satisfies the asymptotic quadratic

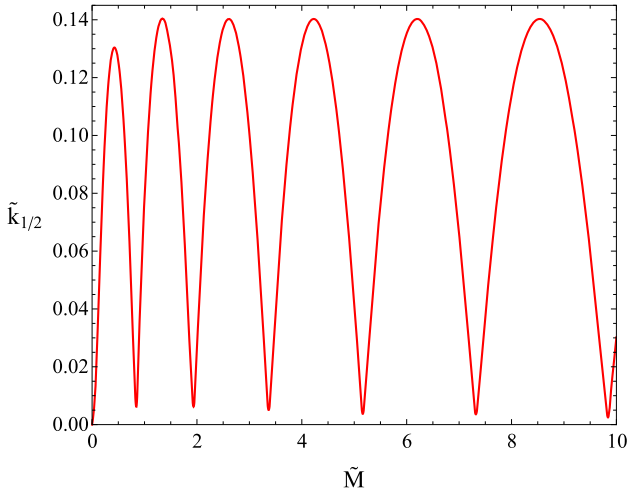

Fig. 6 Dependence of the parameter $\tilde{k}_{1/2}$ on the fermion mass $\tilde{M}$ for the diagonal case

relation

$$\tilde{M}_n \sim an^2, \tag{110}$$

where the coefficient $a \approx 0.18$. It follows that the oscillation period (i.e., the distance between adjacent minima) grows linearly with i:

$$\Delta\tilde{M}_n = \tilde{M}_n - \tilde{M}_{n-1} \sim 2an. \tag{111}$$

From Eqs. (61) and (68), we can find numerical values for the phase shifts for the antidiagonal and diagonal fermionic scattering states. It was found that in the antidiagonal case, the phase shift Δ_{a} does not depend on $\tilde{M}$ and is equal to $\pi/2$. In contrast, in the diagonal case, the phase shift Δ_{d} increases step-wise by π when the fermion mass $\tilde{M}$ passes the next minimum in the curve $\tilde{k}_{1/2}(\tilde{M})$ shown in Fig. 6. Thus, the dependences of the phase shifts on the fermion mass $\tilde{M}$ are described by the expressions:

$$\Delta_{\mathrm{a}}(\tilde{M}) = \frac{\pi}{2}, \tag{112}$$

$$\Delta_{\mathrm{d}}(\tilde{M}) = \pi\left[\frac{1}{2} + \sum_{n=1}^{\infty}\theta(\tilde{M} - \tilde{M}_n)\right], \tag{113}$$

where θ is the Heaviside function and $\tilde{M}_1 \approx 0.85$ is the minimum of the function $\tilde{k}_{1/2}(\tilde{M})$ in Fig. 6 that is nearest to $\tilde{M} = 0$. Levinson's theorem (96) and Eq. (112) tell us that for all values of the fermion mass $\tilde{M}$, there is only one antidiagonal fermionic bound state in the external field of the sine-Gordon kink. On the other hand, according to Levinson's theorem (96) and Eq. (113), the number of diagonal fermionic bound states increases step-wise with an increase in $\tilde{M}$, and there is always at least one diagonal fermionic bound state in the external field of the sine-Gordon kink.

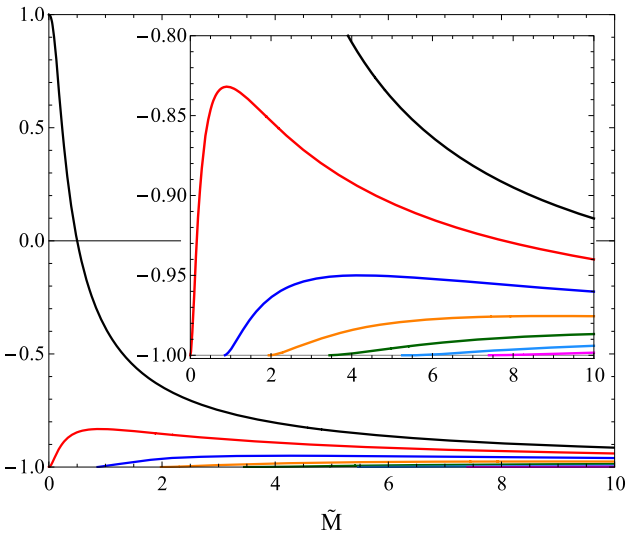

Fig. 7 Dependence of the ratio $\tilde{\varepsilon}/\tilde{M}$ for the antidiagonal bound states of the Dirac Hamiltonian on the fermion mass $\tilde{M}$

In order to verify the validity of these statements, we need to investigate the spectrum of bound states of the Dirac Hamiltonian. It is sufficient to study the spectrum of the antidiagonal component of the Dirac Hamiltonian, since for a given value of $\tilde{M}$, the energy eigenvalues of the diagonal bound states are opposite in sign to those of the antidiagonal bound states. To calculate the energy eigenvalues of the antidiagonal bound states, we used the numerical methods provided by the MATHEMATICA software package [57]. Figure 7 presents the dependence of the ratio $\tilde{\varepsilon}/\tilde{M}$ for the antidiagonal bound states of the Dirac Hamiltonian on the fermion mass $\tilde{M}$. The corresponding curves for the diagonal bound states are obtained from those shown in Fig. 7 by reflection with respect to the horizontal zero axis.

Let us examine the main features of the curves shown in Fig. 7. Firstly, we see that there is only one antidiagonal fermionic bound state in the entire interval of fermion masses $\tilde{M}$. When $\tilde{M} \equiv M/m = 1/2$, the energy of this bound state is zero, and thus the sine-Gordon kink possesses a fermionic zero mode as described in Sect. 4. Conversely, we see that as the fermion mass $\tilde{M}$ increases, new antidiagonal antifermionic bound states arise in the external field of the sine-Gordon kink, and one antidiagonal antifermionic bound state exists for all values of $\tilde{M}$. The situation is reversed for the diagonal bound states. In this case, there is only one diagonal antifermionic bound state, whereas new diagonal fermionic bound states arise as $\tilde{M}$ increases. When $\tilde{M} \equiv M/m = 1/2$, the energy of the diagonal antifermionic bound state vanishes, and it turns into the antifermionic zero mode. The coordinates $\tilde{M}_n$ of the points at which new antidiagonal antifermionic (diagonal fermionic) bound states arise from the continuum coincide with the coordinates of the corresponding minima of the curve $\tilde{k}_{1/2}(\tilde{M})$ in Fig. 6. It was found that in Fig. 7, the curves $|\tilde{\varepsilon}_n|/\tilde{M}$ tend quadratically to unity as $\tilde{M}$ tends to $\tilde{M}_n$ from the right:

$$\frac{|\tilde{\varepsilon}_n|}{\tilde{M}} \approx 1 - \beta_n\big(\tilde{M} - \tilde{M}_n\big)^2, \tag{114}$$

where β_n are some positive constants and the index $n = 0, 1, 2, \ldots$ enumerates the curves in order of increasing $\tilde{M}_n$. A qualitative explanation of this behavior of the curves $|\tilde{\varepsilon}_n|/\tilde{M}$ is given in the Appendix B.

It follows from the above that Eqs. (112), (113), and the the behavior of the curves in Figs. 3, 6, and 7 are in agreement with Levinson's theorem. Indeed, it follows from Eq. (113) that in the scattering of the diagonal state fermions, the phase shift $\Delta_{\rm d}$ increases step-wise by π when $\tilde{M}$ passes the point $\tilde{M}_n$ at which a new diagonal fermionic bound state arises from the continuum. At the same time, in Fig. 6, the curve $\tilde{k}_{1/2}(\tilde{M})$ reaches a local near-zero minimum at $\tilde{M} = \tilde{M}_n$. This corresponds to the fact that diagonal state fermions with $\tilde{M} \approx \tilde{M}_n$ and small momenta $\tilde{k}$ almost completely transmit through the kink barrier. This resonance behavior is due to the presence of a virtual level at $\tilde{k} \approx 0$ when $\tilde{M} \approx \tilde{M}_n$, and is in accordance with the general principles of scattering theory [52–54].

In contrast, it follows from Eq. (112) that in the scattering of the antidiagonal state fermions, the phase shift $\Delta_{\rm a}$ does not depend on $\tilde{M}$ and is equal to $\pi/2$. From Fig. 3, we see that the corresponding curve $\tilde{k}_{1/2}(\tilde{M})$ increases monotonically with an increase in $\tilde{M}$ and has no local minima at nonzero $\tilde{M}$. Hence, the scattering of the antidiagonal state fermions on the sine-Gordon kink does not have a resonance character. This corresponds to the fact that in the external field of the sine-Gordon kink, there are no antidiagonal fermionic states arising at nonzero $\tilde{M}$ and there is only one such state arising at $\tilde{M} = 0$. In addition, we note that the roles of the diagonal and antidiagonal states are reversed when passing from fermions to antifermions. The diagonal (antidiagonal) antifermionic states are scattered on the sine-Gordon kink in the same way as the antidagonal (diagonal) fermionic states.

6 Conclusion

In the present paper, fermion scattering in the background field of the sine-Gordon kink has been investigated both analytically and numerically. To achieve symmetry of the fermion-kink interaction under discrete transformation (3), we treat the sine-Gordon model as a nonlinear σ-model with a circular target space, which interacts with a fermionic isodoublet through the Yukawa interaction. It was found that with respect to its spin and isospin indices, the fermionic isodoublet can be divided into diagonal and antidiagonal parts that

interact with the sine-Gordon kink independently of each other.

Studying the fermion-kink scattering, we have found analytical expressions for the wave functions of the diagonal and antidiagonal fermionic states, and have shown that these wave functions can be expressed in terms of the Heun functions. Using the expressions obtained in this way and the matching conditions for the fermionic wave functions, we have derived general expressions for the fermionic transmission and reflection coefficients. It was found that the scattering of the diagonal fermionic states differs significantly from that of the antidiagonal states. In particular, for the diagonal fermionic states, the dependence of the transmission and reflection coefficients on the fermion mass has an oscillatory resonance character. In contrast, this dependence has a monotonic nonresonance character for the antidiagonal fermionic states. For antifermions the situation is reversed: the scattering of the antidiagonal (diagonal) antifermionic states has a resonance (nonresonance) character.

In general, we can say that the sine-Gordon kink is more transparent for the diagonal fermionic states than for the antidiagonal ones. In particular, it follows from Fig. 6 that the kink becomes transparent ($T \approx 1$) for the diagonal fermions in the entire range of the fermion mass $\tilde{M}$ already at $\tilde{k} \gtrsim 0.3$. Moreover, the kink becomes transparent at extremely small values of the fermion momentum $\tilde{k}$ at the resonance values of $\tilde{M}$. In contrast, we can see from Fig. 3 that for the antidiagonal fermions, the transparency of the kink comes at much higher values of the fermion momentum $\tilde{k}$.

The fermion-kink system has a rather interesting structure of the bound states. Their energy levels are determined by zeros of the coefficient of the incident wave in the asymptotics of the fermionic scattering states. The number of bound states increases as the Yukawa coupling g constant increases, which is equivalent to an increase in the fermion mass M. The growth in the number of bound states is asymptotically $\propto M^{1/2} = m^{1/2} g^{1/2} \lambda^{-1/4}$. At the same time, for any nonzero M, there are at least four bound states, of which two are fermionic and two are antifermionic. The diagonal fermionic (antifermionic) bound states are related by the charge conjugation to the antidiagonal antifermionic (fermionic) bound states, meaning that the energy levels of the fermion-kink system can be divided into pairs of levels with opposite energies.

In addition, the fermion-kink system will possesses two zero modes when condition (79) is satisfied. Of these, the antidiagonal zero mode is fermionic, while the diagonal one is antifermionic, and these modes are related by the charge conjugation. The two linear combinations of the fermionic and antifermionic zero modes are the eigenstates of the charge conjugation operator, and hence are the Majorana zero modes. The Majorana zero modes have no effect on the field configuration of the sine-Gordon kink.

It should be noted that as the fermion mass M increases, the number of the antidiagonal fermionic (diagonal antifermionic) states remains equal to one, while the number of the antidiagonal antifermionic (diagonal fermionic) states increases asymptotically $\propto M^{1/2}$. This difference in the properties of the bound states appears to be closely related through Levinson's theorem to the above-mentioned difference in the scattering of the diagonal and antidiagonal states on the sine-Gordon kink.

In addition to the sine-Gordon kink, there is the well-known kink solution of the $(1 + 1)$-dimensional ϕ^4 model [3–5]. The ϕ^4 kink possesses a single Majorana zero mode, which exists for all nonzero values of the Yukawa coupling constant. This is the main difference from the sine-Gordon kink, which has two zero modes, but only if condition (79) is satisfied. As in the previous case, the Majorana zero mode has no effect on the field configuration of the ϕ^4 kink. The presence of the single Majorana zero mode leads to fragmentation of the fermionic charge and polarization of the fermionic vacuum in the external field of the ϕ^4 kink, for any nonzero value of the Yukawa coupling constant. In contrast, the presence of the two zero modes $\psi_{0\mathrm{a}}$ and $\psi_{0\mathrm{d}}$ in the external field of the sine-Gordon kink makes it possible to form the two Majorana zero modes $\psi_{0\mathrm{e}}$ and $\psi_{0\mathrm{o}}$ in the exceptional case (79). The presence of two zero modes makes fragmentation of the fermionic charge impossible in the external field of the sine-Gordon kink. At the same time, the fermionic charge of the vacuum state $|0, 0\rangle_{(2)}$ is equal to minus one, which indicates polarization of the fermionic vacuum in the subspace of the Majorana zero modes.

As in the case of the sine-Gordon kink, the number of fermionic bound states of the ϕ^4 kink increases with an increase in the fermionic mass M. However, the number of bound fermionic states of the ϕ^4 kink is asymptotically $\propto M$, while that of the sine-Gordon kink is asymptotically $\propto M^{1/2}$. Hence, we can say that the ϕ^4 kink holds fermions more efficiently than the sine-Gordon kink.

Being embedded in $(3 + 1)$-dimensional space, a kink becomes a domain wall. In particular, domain walls can exist in non-linear $(3 + 1)$-dimensional field models (gauged or non-gauged) with the target space being a sphere S^2. We believe that the characteristic features of the fermion-sG kink scattering are preserved in this case. Suppose that the cloud of fermionic gas is to the left of the domain wall at an initial instant of time, and concentrations of the diagonal and antidiagonal fermionic states (which we denote by n_{d} and n_{a}, respectively) are the same. Then after some time interval, $n_{\mathrm{a}} > n_{\mathrm{d}}$ to the left of the domain wall and $n_{\mathrm{a}} < n_{\mathrm{d}}$ to the right of it. It follows that the fermion gas becomes spin-isospin correlated to the left of the domain wall. A similar situation takes place for the fermion gas to the right of the wall, but in this case, the sign of the spin-isospin correlation will be opposite. The diagonal and antidiagonal fermionic states interact

differently with gauge and scalar fields, and the d-d fermion scattering is different from the a-a fermion scattering. It follows that the difference in the interactions of the diagonal and antidiagonal fermionic states with the domain wall can play an important role in cosmological models that allow the existence of such domain walls.

As noted above, all the results related to the fermion-kink system are valid only if conditions (21) and (22) hold. This applies to both scattering and bound states of the fermion-kink system. Consideration of bosonic and fermionic quantum corrections modifies the results obtained. The corresponding corrections are on the order of λm^{-2} and $g^2 m^{-2}$, respectively. Taking into account the fermion backreaction leads to the corrections on the order of $g m^{-2}\lambda^{1/2}$. It follows that in the strong coupling regime, in which $\lambda m^{-2} \gtrsim 1$ and/or $g^2 m^{-2} \gtrsim 1$, the correction terms will be of the same order as the basic terms, and therefore the results obtained become inapplicable.

Acknowledgements This research was funded by the Ministry of Science and Higher Education of Russia, Government Order for 2020-2022, project no. FEWM-2020-0037 (TUSUR).

Data Availability Statement This manuscript has no associated data or the data will not be deposited. [Authors' comment: This paper does not use any additional data.]

Funded by SCOAP[3]. SCOAP[3] supports the goals of the International Year of Basic Sciences for Sustainable Development.

Appendix A: Plane-wave solutions to the Dirac equation

When $|x| \gg m^{-1}$, the Dirac equation (9) describing fermions in external kink field (12) turns into the free Dirac equation

$$i\gamma^\mu \otimes \mathbb{I}\partial_\mu \psi - M\mathbb{I} \otimes \tau_1 \psi = 0, \tag{A.1}$$

where the fermion mass $M = mg\lambda^{-1/2}$, and we explicitly write out the matrices acting on the spinor and isospinor indices. The free Dirac Hamiltonian corresponding to Eq. (A.1) is

$$H_0 = \alpha \otimes \mathbb{I}\,(-i\partial_x) + M\beta \otimes \tau_1, \tag{A.2}$$

where $\alpha = \gamma^0\gamma^1$ and $\beta = \gamma^0$. The Hamiltonian (A.2) commutes with the operators $p_x = -i\partial_x$ and $I_1 = 2^{-1}\tau_1$ corresponding to the momentum and isospin x-projection of a free fermion, respectively. It follows that the states of free fermions can be characterized by the momentum p_x and isospin x-projection I_1. Since in the one-dimensional case fermions have no spin, there exist four fermionic states at a fixed fermion momentum p_x. These states correspond to the combinations of the isospin x-projections $I_1 = \pm 1/2$ and the fermion energies $p_0 = \pm\varepsilon = \pm(p_x^2 + M^2)^{1/2}$ with both signs.

Let us denote the wave function of a fermion with momentum p_x, energy $p_0 = \epsilon\left(p_x^2 + M^2\right)^{1/2}$, where $\epsilon = \pm 1$, and isospin x-projection I_x by ψ_{p_x,ϵ,I_1}. Then, the wave functions of free fermions have the form

$$\psi_{p_x,1,1/2} = \frac{1}{2\sqrt{\varepsilon L}}\begin{pmatrix}\sqrt{\varepsilon+p_x} & \sqrt{\varepsilon+p_x}\\ \sqrt{\varepsilon-p_x} & \sqrt{\varepsilon-p_x}\end{pmatrix} \times \exp[-i\,(\varepsilon t - p_x x)], \tag{A.3a}$$

$$\psi_{p_x,-1,1/2} = \frac{1}{2\sqrt{\varepsilon L}}\begin{pmatrix}-\sqrt{\varepsilon-p_x} & -\sqrt{\varepsilon-p_x}\\ \sqrt{\varepsilon+p_x} & \sqrt{\varepsilon+p_x}\end{pmatrix} \times \exp[i\,(\varepsilon t + p_x x)], \tag{A.3b}$$

$$\psi_{p_x,1,-1/2} = \frac{1}{2\sqrt{\varepsilon L}}\begin{pmatrix}-\sqrt{\varepsilon+p_x} & \sqrt{\varepsilon+p_x}\\ \sqrt{\varepsilon-p_x} & -\sqrt{\varepsilon-p_x}\end{pmatrix} \times \exp[-i\,(\varepsilon t - p_x x)], \tag{A.3c}$$

$$\psi_{p_x,-1,-1/2} = \frac{1}{2\sqrt{\varepsilon L}}\begin{pmatrix}\sqrt{\varepsilon-p_x} & -\sqrt{\varepsilon-p_x}\\ \sqrt{\varepsilon+p_x} & -\sqrt{\varepsilon+p_x}\end{pmatrix} \times \exp[i\,(\varepsilon t + p_x x)], \tag{A.3d}$$

where L is the normalized length. In Eqs. (A.3a)–(A.3d), the first (second) index of the matrices corresponds to the spinor (isospinor) structure of the fermionic wave function. The wave functions ψ_{p_x,ϵ,I_1} satisfy the normalized relations:

$$\bar\psi_{p_x,\epsilon,I_1}\gamma^\mu\psi_{p_x,\epsilon,I_1} = \left(1, \epsilon p_x \varepsilon^{-1}\right) = (1, \epsilon v_x), \tag{A.4a}$$

$$\bar\psi_{\epsilon p_x,\epsilon,I_1}\gamma^\mu\psi_{\epsilon p_x,\epsilon,I_1} = \left(1, p_x\varepsilon^{-1}\right) = (1, v_x), \tag{A.4b}$$

$$\bar\psi_{p_x,\epsilon,I_1}\psi_{p_x,\epsilon,I_1} = (-1)^{1/2-I_1}\,\epsilon M\varepsilon^{-1}, \tag{A.4c}$$

where the normalized length L is taken to be equal to unity.

Let us define the spinor-isospinor amplitude u_{p_x,ϵ,I_1} of the fermionic wave function ψ_{p_x,ϵ,I_1} by the relation $\psi_{p_x,\epsilon,I_1} \equiv (2\varepsilon L)^{-1/2}\,u_{p_x,\epsilon,I_1}\exp\left[-i\,(\epsilon\varepsilon t - p_x x)\right]$. Then, the amplitudes u_{p_x,ϵ,I_1} satisfy the orthogonality and completeness relations:

$$u^\dagger_{p_x,\epsilon,I_1}u_{p_x,\epsilon',I_1'} = 2\varepsilon\delta_{\epsilon,\epsilon'}\delta_{I_1,I_1'}, \tag{A.5a}$$

$$\sum_{\epsilon,\,I_1} u_{p_x,\epsilon,I_1[i,a]}u^\dagger_{p_x,\epsilon,I_1[j,b]} = 2\varepsilon\delta_{i,j}\delta_{a,b} \tag{A.5b}$$

for the Hermitian conjugate case, and

$$\bar u_{\epsilon p_x,\epsilon,I_1}u_{\epsilon' p_x,\epsilon',I_1'} = 2M\epsilon\,(-1)^{1/2-I_1}\,\delta_{\epsilon,\epsilon'}\delta_{I_1,I_1'}, \tag{A.6a}$$

$$\sum_{I_1} u_{\epsilon p_x,\epsilon,I_1[i,a]}\bar{u}_{\epsilon p_x,\epsilon,I_1[j,b]} = \left\{\gamma^\mu p_\mu + \epsilon M\right\}_{i,j}\delta_{a,b}, \tag{A.6b}$$

$$\sum_{\epsilon,\, I_1} \epsilon u_{\epsilon p_x,\epsilon,I_1[i,a]}\bar{u}_{\epsilon p_x,\epsilon,I_1[j,b]} = 2M\delta_{i,j}\delta_{a,b} \tag{A.6c}$$

for the Dirac conjugate case. In Eqs. (A.5b), (A.6b), and (A.6c), the first (second) index in square brackets is the spinor (isospinor) one.

As for the Dirac equation (9), the free Dirac equation (A.1) is invariant under the C, P, and T transformations (15a)–(15c). However, it is also invariant under the additional variants of these transformations:

$$\psi^{C'}(t,x) = \eta_{C'}\gamma_5 \otimes \mathbb{I}\psi^*(t,x), \tag{A.7a}$$
$$\psi^{C''}(t,x) = \eta_{C''}\mathbb{I} \otimes \tau_2\psi^*(t,x), \tag{A.7b}$$
$$\psi^{C'''}(t,x) = \eta_{C'''}\mathbb{I} \otimes \tau_3\psi^*(t,x), \tag{A.7c}$$
$$\psi^{P'}(t,x) = \eta_{P'}\gamma^0 \otimes \mathbb{I}\psi(t,-x), \tag{A.7d}$$
$$\psi^{T'}(t,x) = \eta_{T'}\gamma^0 \otimes \mathbb{I}\psi^*(-t,x). \tag{A.7e}$$

In particular, it follows from Eqs. (A.7b) and (A.7c) that

$$\psi_{p_x,\epsilon,I_1} \xrightarrow{C''} (-1)^{(I_1+1)/2}\psi_{-p_x,-\epsilon,-I_1}, \tag{A.8a}$$
$$\psi_{p_x,\epsilon,I_1} \xrightarrow{C'''} \psi_{-p_x,-\epsilon,-I_1}, \tag{A.8b}$$

where the phase factors $\eta_{C''}$ and $\eta_{C'''}$ are taken equal to $-i$ and 1, respectively. It follows that in the second quantization formalism, the negative frequency fermionic wave function $\psi_{-p_x,-1,-I_1}$ can be used to describe the antifermion having the momentum p_x and isospin x-projection I_1.

The free Hamiltonian (A.2) commutes with the operator $T_3 = \gamma_5 \otimes \tau_3$, which determines the type (diagonal or antidiagonal) of the state. At the same time, the operator T_3 does not commute with the isospin operator $I_1 = 2^{-1}\mathbb{I}\otimes\tau_1$. It follows that the eigenstates of the operator T_3 are linear combinations of the eigenstates of the isospin operator I_1:

$$\psi_{p_x,1,\mathrm{d}} = 2^{-1/2}\left(\psi_{p_x,1,1/2} - \psi_{p_x,1,-1/2}\right), \tag{A.9a}$$
$$\psi_{p_x,1,\mathrm{a}} = 2^{-1/2}\left(\psi_{p_x,1,1/2} + \psi_{p_x,1,-1/2}\right), \tag{A.9b}$$
$$\psi_{p_x,-1,\mathrm{d}} = 2^{-1/2}\left(\psi_{p_x,-1,1/2} - \psi_{p_x,-1,-1/2}\right), \tag{A.9c}$$
$$\psi_{p_x,-1,\mathrm{a}} = 2^{-1/2}\left(\psi_{p_x,-1,1/2} + \psi_{p_x,-1,-1/2}\right). \tag{A.9d}$$

Appendix B: Energy of a bound fermionic (antifermionic) state in the vicinity of the transition to the continuum

In this appendix, we explain the behavior of the curves $|\varepsilon_n|/M$ expressed by Eq. (114). Since for the diagonal and antidiagonal cases the curves $|\varepsilon_n(M)|$ are the same, we shall consider only the diagonal case. As M tends to M_n from the right, the curve $|\varepsilon_n(M)|/M$ tends to unity. It follows that in this case, the parameter $\kappa = \left(M^2 - \varepsilon^2\right)^{1/2}$ tends to zero.

Let us replace the independent variable x in the differential equation (30) by $\xi = \kappa x$. After this replacement, the differential equation takes the form

$$\psi_{11}''(\xi) + 2im\kappa^{-1}\mathrm{sech}\left(m\kappa^{-1}\xi\right)\psi_{11}'(\xi) - \left(1 - 2\varepsilon m\kappa^{-2}\mathrm{sech}\left(m\kappa^{-1}\xi\right)\right)\psi_{11}(\xi) = 0. \tag{B.1}$$

When the dimensionless variable $|\xi| \gg \kappa m^{-1}$, the function $\mathrm{sech}\left(m\kappa^{-1}\xi\right)$ exponentially tends to zero. In this case, we can neglect the corresponding terms in Eq. (B.1) and find that

$$\psi_{11}(\xi) \propto \exp(-|\xi|) \tag{B.2}$$

when $|\xi| \gg \kappa m^{-1}$. Next we turn to the region of $|\xi| \ll \kappa m^{-1}$, where the function $\mathrm{sech}\left(m\kappa^{-1}\xi\right)$ can be set equal to unity. Using this fact, we find an approximate solution to Eq. (B.1) in the region of $|\xi| \ll \kappa m^{-1}$:

$$\psi_{11}(\xi) \propto \exp\left(-i\kappa^{-1}\tau\xi\right), \tag{B.3}$$

where the parameter

$$\tau = m + \epsilon\left(m^2 + 2m\varepsilon - \kappa^2\right)^{1/2} \tag{B.4}$$

and $\epsilon = \pm 1$.

Now we need to match solutions (B.2) and (B.3) at $\xi = \kappa m^{-1}$. Since, for $|\xi| \ll \kappa m^{-1}$, Eq. (B.1) contains the imaginary coefficient $2im\kappa^{-1}$, solution (B.3) is essentially complex. The matching condition must be satisfied for both the real and imaginary parts of solution (B.3). Let us consider the real part of Eq. (B.3):

$$\mathrm{Re}\left[\psi_{11}(\xi)\right] \propto \cos\left(\kappa^{-1}\tau\xi\right). \tag{B.5}$$

By equating the logarithmic derivatives of Eqs. (B.2) and (B.5) at $\xi = \kappa m^{-1}$, we arrive at the transcendental equation

$$\tau\tan\left(m^{-1}\tau\right) = \kappa. \tag{B.6}$$

From Eq. (B.6) it follows that $\tan\left(m^{-1}\tau\right)$ must tend to zero together with κ. This, in turn, implies that the combination $m^{-1}\tau$ can be written as

$$m^{-1}\tau = \pi n + \Delta, \tag{B.7}$$

where n is a nonnegative integer and $\Delta \to 0$ as $\kappa \to 0$. Combining Eqs. (B.4) and (B.7), we find that

$$|\varepsilon_n| \underset{\kappa\to 0}{\longrightarrow} M_n = m\pi n\left(n\pi/2 - 1\right), \tag{B.8}$$

where ε_n is the energy of the n-th fermionic (antifermionic) bound state. We see that for large n, the value of the fermion mass at which the n-th fermionic (antifermionic) bound state arises from the continuum becomes approximately proportional to n^2. Note that this fact is in accordance with Eqs. (110) and (111).

By substituting Eq. (B.7) into Eq. (B.6), we obtain the transcendental equation in terms of the parameters Δ and κ:

$$m\left(\pi n+\Delta\right)\tan\left(\Delta\right)=\kappa. \tag{B.9}$$

We now study the behavior of the curve $|\varepsilon_n(M)|$ in the neighborhood of the fermion mass M_n, where both Δ and κ tend to zero. Expanding the right-hand side of Eq. (B.9) in terms of Δ and keeping the first expansion terms, we obtain the equation

$$mn\pi\,\Delta\left(1-\delta_{n0}\right)+m\Delta^2\delta_{n0}=\kappa. \tag{B.10}$$

In Eq. (B.10), we can express both Δ and κ in terms of ε and M, using Eqs. (B.4), (B.7), and the definition $\kappa=\left(M^2-\varepsilon^2\right)^{1/2}$. In the neighborhood of M_n (defined in Eq. (B.8)), the variables ε and M can be written as

$$\varepsilon=M_n+\Delta\varepsilon, \tag{B.11a}$$
$$M=M_n+\Delta M. \tag{B.11b}$$

As a result, we obtain a cumbersome expression implicitly defining $\Delta\varepsilon$ as a function of ΔM in the neighborhood of M_n:

$$F\left(m,n,\Delta M,\Delta\varepsilon\right)=0. \tag{B.12}$$

The value of $\Delta\varepsilon$ should vanish along with that of ΔM, and therefore Eq. (B.12) must be satisfied identically when $\Delta\varepsilon$ and ΔM vanish. This can be used to determine the sign factor ϵ in Eq. (B.4):

$$\epsilon=1-2\delta_{n0}, \tag{B.13}$$

where it is understood that in Eq. (B.4), the principal value of the square root is used.

Using expression (B.12), treating $\Delta\varepsilon$ as a function of ΔM, and applying the rules for differentiation of an implicit function, we obtain sequentially:

$$\Delta\varepsilon\left(0\right)=0, \tag{B.14a}$$
$$\Delta\varepsilon'\left(0\right)=1, \tag{B.14b}$$
$$\Delta\varepsilon''\left(0\right)=-\frac{2\pi n}{m\left(\pi n-2\right)\left(\pi n-1\right)^2}, \tag{B.14c}$$
$$\Delta\varepsilon'''\left(0\right)=\frac{6}{m^2}\frac{-2+4\pi n-\pi^2n^2+\pi^2n^3}{\left(\pi n-2\right)^2\left(\pi n-1\right)^3}. \tag{B.14d}$$

for $n=1,2,3,\ldots$, and

$$\Delta\varepsilon\left(0\right)=0, \tag{B.15a}$$
$$\Delta\varepsilon'\left(0\right)=\pm1, \tag{B.15b}$$
$$\Delta\varepsilon''\left(0\right)=0, \tag{B.15c}$$
$$\Delta\varepsilon'''\left(0\right)=\mp3m^{-2} \tag{B.15d}$$

for $n=0$. The two signs in Eqs. (B.15b) and (B.15d) correspond to the two curves starting at $\tilde{M}=0$ in Fig. 7.

It follows from Eqs. (B.14) and (B.15) that $\left|\Delta\varepsilon'\left(0\right)\right|$ is exactly equal to one and that $\Delta\varepsilon''\left(0\right)$ vanishes when $n=0$. We can show that this behavior of the function $\Delta\varepsilon\left(\Delta M\right)$ corresponds to Eq. (114). To do this, we suppose that in the neighborhood of M_n, the function $|\varepsilon_n|/M$ has the form

$$\frac{|\varepsilon_n|}{M}=1-\alpha_n\left(M-M_n\right)-\beta_n\left(M-M_n\right)^2 -\gamma_n\left(M-M_n\right)^3+O\left[\left(M-M_n\right)^4\right], \tag{B.16}$$

where α_n, β_n, and γ_n are constant coefficients. Rewriting Eq. (B.16) in terms of $\Delta\varepsilon=|\varepsilon_n|-M_n$ and $\Delta M=M-M_n$, we obtain the expression

$$\Delta\varepsilon=\left(1-M_n\alpha_n\right)\Delta M-\left(\alpha_n+M_n\beta_n\right)\Delta M^2 -\left(\beta_n+M_n\gamma_n\right)\Delta M^3+O\left(\Delta M^4\right). \tag{B.17}$$

From Eqs. (B.14) and (B.15) it follows that in Eq. (B.17), the coefficient α_n vanishes, whereas the coefficient $\beta_n\neq0$ and is positive for all n. Under these conditions, Eqs. (114) and (B.16) become equivalent. Note also that in Eq. (B.17), the coefficient at ΔM^2 vanishes when $n=0$, in accordance with Eq. (B.15c).

We conclude that the use of the rather rough approximation allows us to explain the behavior of the curves in Fig. 7 at a qualitative level.

References

1. N. Manton, P. Sutclffe, *Topological Solitons* (Cambridge University Press, Cambridge, 2004)
2. T. Vachaspati, *Kinks and Domain Walls* (Cambridge University Press, Cambridge, 2006)
3. R. F. Dashen, B. Hasslacher, A. Neveu, Phys. Rev. D **10**, 4130 (1974). https://doi.org/10.1103/PhysRevD.10.4130
4. A.M. Polyakov, JETP Lett. **20**, 194 (1974)
5. J. Goldstone, R. Jackiw, Phys. Rev. D **11**, 1486 (1975). https://doi.org/10.1103/PhysRevD.11.1486
6. T.H.R. Skyrme, Proc. R. Soc. Lond. A **262**, 237 (1961). https://doi.org/10.1098/rspa.1961.0115
7. T.H.R. Skyrme, Nucl. Phys. **31**, 556 (1962). https://doi.org/10.1016/0029-5582(62)90775-7
8. S. Coleman, Phys. Rev. D **11**, 2088 (1975). https://doi.org/10.1103/PhysRevD.11.2088
9. H. Blas, H.L. Carrion, JHEP **01**, 027 (2007). https://doi.org/10.1088/1126-6708/2007/01/027
10. H. Blas, JHEP **03**, 055 (2007). https://doi.org/10.1088/1126-6708/2007/03/055

11. M. Nitta, Phys. Rev. D **87**, 025013 (2013). https://doi.org/10.1103/PhysRevD.87.025013
12. A. Barone, G. Paterno, *Physics and Applications of the Josephson Effect* (Wiley Interscience, New York, 1982)
13. A. Davidson, B. Dueholm, B. Kryger, N.F. Pedersen, Phys. Rev. Lett. **55**, 2059 (1985). https://doi.org/10.1103/PhysRevLett.55.2059
14. E. Goldobin, A. Wallraff, N. Thyssen, A.V. Ustinov, Phys. Rev. B **57**, 130 (1998). https://doi.org/10.1103/PhysRevB.57.130
15. I. Nandori, U.D. Jentschura, S. Nagy, K. Sailer, K. Vad, S. Meszaros, J. Phys.: Condens. Matter **19**, 236226 (2007)
16. I. Nandori, K. Vad, S. Meszaros, U.D. Jentschura, S. Nagy, K. Sailer, J. Phys.: Condens. Matter **19**, 496211 (2007). https://doi.org/10.1088/0953-8984/19/23/236226
17. L. Benfatto, C. Castellani, T. Giamarchi, Phys. Rev. Lett. **98**, 117008 (2007). https://doi.org/10.1103/PhysRevLett.98.117008
18. J.-S. Caux, H. Saleur, F. Siano, Phys. Rev. Lett. **88**, 106402 (2002). https://doi.org/10.1103/PhysRevLett.88.106402
19. R. Jackiw, C. Rebbi, Phys. Rev. D **13**, 3398 (1976). https://doi.org/10.1103/PhysRevD.13.3398
20. J. Goldstone, F. Wilczek, Phys. Rev. Lett. **47**, 986 (1981). https://doi.org/10.1103/PhysRevLett.47.986
21. R. MacKenzie, F. Wilczek, Phys. Rev. D **30**, 2194 (1984). https://doi.org/10.1103/PhysRevD.30.2194
22. A.J. Niemi, G.W. Semenoff, Phys. Rept. **135**, 99 (1986). https://doi.org/10.1016/0370-1573(86)90167-5
23. E. Witten, Nucl. Phys. B **249**, 557 (1985). https://doi.org/10.1016/0550-3213(85)90022-7
24. V.A. Rubakov, JETP Lett. **33**, 644 (1981)
25. V.A. Rubakov, Nucl. Phys. B **203**, 311 (1982). https://doi.org/10.1016/0550-3213(82)90034-7
26. C.G. Callan, Phys. Rev. D **25**, 2141 (1982). https://doi.org/10.1103/PhysRevD.25.2141
27. C.G. Callan, Phys. Rev. D **26**, 2058 (1982). https://doi.org/10.1103/PhysRevD.26.2058
28. S.S. Gousheh, A. Mohammadi, L. Shahkarami, Eur. Phys. J. C **74**, 3020 (2014). https://doi.org/10.1140/epjc/s10052-014-3020-2
29. M.B. Voloshin, Yad. Fiz. **21**, 1331 (1975)
30. A. Ayala, J. Jalilian-Marian, L. McLerran, A.P. Vischer, Phys. Rev. D **49**, 5559 (1994). https://doi.org/10.1103/PhysRevD.49.5559 10.1103/PhysRevD.49.5559
31. K. Funakubo, A. Kakuto, S. Otsuki, K. Takenaga, F. Toyoda, Phys. Rev. D **50**, 1105 (1994). https://doi.org/10.1103/PhysRevD.50.1105
32. G.R. Farrar, J.W. McIntosh, Phys. Rev. D **51**, 5889 (1995). https://doi.org/10.1103/PhysRevD.51.5889
33. G.R. Farrar, M.E. Shaposhnikov, Phys. Rev. D **50**, 774 (1994). https://doi.org/10.1103/PhysRevD.50.774
34. N. Graham, R.L. Jaffe, Nucl. Phys. B **544**, 432 (1999). https://doi.org/10.1016/S0550-3213(99)00027-9
35. N. Graham, R.L. Jaffe, Nucl. Phys. B **549**, 516 (1999). https://doi.org/10.1016/S0550-3213(99)00148-0
36. D. Stojkovic, Phys. Rev. D **63**, 025010 (2000). https://doi.org/10.1103/PhysRevD.63.025010
37. L. Campanelli, P. Cea, G.L. Fogli, L. Tedesco, Phys. Rev. D **65**, 085004 (2002). https://doi.org/10.1103/PhysRevD.65.085004
38. L. Campanelli, Phys. Rev. D **70**, 116008 (2004). https://doi.org/10.1103/PhysRevD.70.116008
39. G. Gibbons, K.I. Maeda, Y.I. Takamizu, Phys. Lett. B **647**, 1 (2007). https://doi.org/10.1016/j.physletb.2007.01.042
40. Y.Z. Chu, T. Vachaspati, Phys. Rev. D **77**, 025006 (2008). https://doi.org/10.1103/PhysRevD.77.025006
41. Y.X. Liu, L.D. Zhang, L.J. Zhang, Y.S. Duan, Phys. Rev. D **78**, 065025 (2008). https://doi.org/10.1103/PhysRevD.78.065025
42. Y. Brihaye, T. Delsate, Phys. Rev. D **78**, 025014 (2008). https://doi.org/10.1103/PhysRevD.78.025014
43. V.A. Gani, V.G. Ksenzov, A.E. Kudryavtsev, Phys. At. Nucl. **73**, 1889 (2010). https://doi.org/10.1134/S1063778810110104
44. Y. Brihaye, T. Delsate, Phys. Rev. D **86**, 024029 (2012). https://doi.org/10.1103/PhysRevD.86.024029
45. A. Amado, A. Mohammadi, Eur. Phys. J. C **77**, 465 (2017). https://doi.org/10.1140/epjc/s10052-017-5044-x
46. AYu. Loginov, Phys. Rev. D **95**, 065003 (2017). https://doi.org/10.1103/PhysRevD.95.065003
47. V. Klimashonok, I. Perapechka, Ya.. Shnir, Phys. Rev. D **100**, 105003 (2019). https://doi.org/10.1103/PhysRevD.100.105003
48. I. Perapechka, Ya.. Shnir, Phys. Rev. D **101**, 021701(R) (2020). https://doi.org/10.1103/PhysRevD.101.021701
49. R. Rajaraman, *Solitons and Instantons* (Elsevier Science, Amsterdam, 1987)
50. A. Ronveaux (ed.), *Heun's Differential Equations* (Oxford University Press, Oxford, 1995)
51. F.W.J. Olver, D.W. Lozier, R.F. Boisvert, C.W. Clark (eds.), *NIST Handbook of Mathematical Functions* (Cambridge University Press, Cambridge, 2010)
52. L. D. Landau, E. M. Lifshitz, *Quantum Mechanics: Non-Relativistic Theory*, (Pergamon Press, Oxford, 1977), Vol. 3, 3rd ed
53. M.L. Goldberger, K.M. Watson, *Collision Theory* (John Wiley & Sons Inc, New York, 1967)
54. J.R. Taylor, *Scattering Theory: Quantum Theory on Nonrelativistic Collisions* (John Wiley & Sons, New York, 1972)
55. N. Levinson, Danske Vidensk. Selsk. K. Mat.-Fys. Medd. **25**(9) (1949)
56. G. Barton, J. Phys. A: Math. Gen. **18**, 479 (1985). https://doi.org/10.1088/0305-4470/18/3/023
57. Wolfram Research, Inc., Mathematica, Version 12.2. Champaign, IL (2020). https://www.wolfram.com